3-6-2018

α Cell Function and Gene Expression Are Compromised in Type 1 Diabetes.

Marcela Brissova

Rachana Haliyur

Diane Saunders

Shristi Shrestha

Chunhua Dai

See next page for additional authors

Authors
Marcela Brissova, Rachana Haliyur, Diane Saunders, Shristi Shrestha, Chunhua Dai, David M Blodgett, Rita Bottino, Martha Campbell-Thompson, Radhika Aramandla, Gregory Poffenberger, Jill Lindner, Fong Cheng Pan, Matthias G von Herrath, Dale L Greiner, Leonard D. Shultz, May Sanyoura, Louis H Philipson, Mark Atkinson, David M Harlan, Shawn E Levy, Nripesh Prasad, Roland Stein, and Alvin C Powers

Article

Cell Reports

α Cell Function and Gene Expression Are Compromised in Type 1 Diabetes

Graphical Abstract

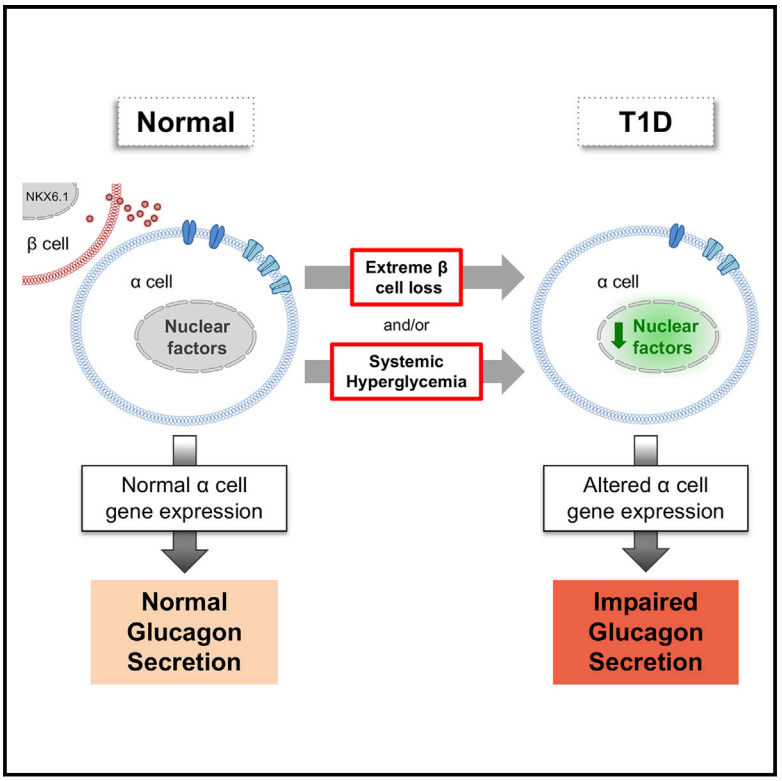

Authors

Marcela Brissova, Rachana Haliyur, Diane Saunders, ..., Nripesh Prasad, Roland Stein, Alvin C. Powers

Correspondence

marcela.brissova@vanderbilt.edu (M.B.), al.powers@vanderbilt.edu (A.C.P.)

In Brief

Brissova et al. find that β cells in the type 1 diabetic (T1D) pancreas maintain several functional and molecular features, but α cells have impaired glucagon secretion and an altered gene expression profile. These findings provide insight into the mechanism of α cell dysfunction in T1D.

Highlights

- T1D β cells appear to maintain several aspects of regulated insulin secretion
- T1D α cells have impaired glucagon secretion and altered gene expression
- Unlike in rodents, α-to-β cell conversion in human T1D is a very rare event
- T1D α cell identity factors improve in a non-autoimmune, normoglycemic environment

Data and Software Availability

GSE106148

Brissova et al., 2018, Cell Reports 22, 2667–2676
March 6, 2018
https://doi.org/10.1016/j.celrep.2018.02.032

CellPress

Cell Reports
Article

α Cell Function and Gene Expression Are Compromised in Type 1 Diabetes

Marcela Brissova,[1,13,*] Rachana Haliyur,[2,13] Diane Saunders,[2,13] Shristi Shrestha,[3,13] Chunhua Dai,[1] David M. Blodgett,[4,5] Rita Bottino,[6] Martha Campbell-Thompson,[7] Radhika Aramandla,[1] Gregory Poffenberger,[1] Jill Lindner,[1] Fong Cheng Pan,[8] Matthias G. von Herrath,[9] Dale L. Greiner,[4] Leonard D. Shultz,[10] May Sanyoura,[11] Louis H. Philipson,[11] Mark Atkinson,[7] David M. Harlan,[4] Shawn E. Levy,[3] Nripesh Prasad,[3] Roland Stein,[1,8] and Alvin C. Powers[1,2,12,14,*]

[1]Department of Medicine, Division of Diabetes, Endocrinology and Metabolism, Vanderbilt University Medical Center, Nashville, TN, USA
[2]Department of Molecular Physiology and Biophysics, Vanderbilt University, Nashville, TN, USA
[3]HudsonAlpha Institute for Biotechnology, Huntsville, AL, USA
[4]Department of Medicine, Diabetes Division, Diabetes Center of Excellence, University of Massachusetts Medical School, Worcester, MA, USA
[5]Math and Science Division, Babson College, Wellesley, MA 02457, USA
[6]Institute of Cellular Therapeutics, Allegheny-Singer Research Institute, Allegheny Health Network, Pittsburgh, PA, USA
[7]Department of Pathology, University of Florida Diabetes Institute, College of Medicine, Gainesville, FL, USA
[8]Department of Cell and Developmental Biology, Vanderbilt University, Nashville, TN, USA
[9]Type 1 Diabetes Center, the La Jolla Institute for Allergy and Immunology, La Jolla, CA, USA
[10]The Jackson Laboratory, Bar Harbor, ME, USA
[11]Departments of Medicine and Pediatrics, Section of Endocrinology, Diabetes, and Metabolism, University of Chicago, Chicago, IL, USA
[12]Department of Veterans Affairs, Tennessee Valley Healthcare System, Nashville, TN, USA
[13]These authors contributed equally
[14]Lead Contact
*Correspondence: marcela.brissova@vanderbilt.edu (M.B.), al.powers@vanderbilt.edu (A.C.P.)
https://doi.org/10.1016/j.celrep.2018.02.032

SUMMARY

Many patients with type 1 diabetes (T1D) have residual β cells producing small amounts of C-peptide long after disease onset but develop an inadequate glucagon response to hypoglycemia following T1D diagnosis. The features of these residual β cells and α cells in the islet endocrine compartment are largely unknown, due to the difficulty of comprehensive investigation. By studying the T1D pancreas and isolated islets, we show that remnant β cells appeared to maintain several aspects of regulated insulin secretion. However, the function of T1D α cells was markedly reduced, and these cells had alterations in transcription factors constituting α and β cell identity. In the native pancreas and after placing the T1D islets into a non-autoimmune, normoglycemic *in vivo* environment, there was no evidence of α-to-β cell conversion. These results suggest an explanation for the disordered T1D counterregulatory glucagon response to hypoglycemia.

INTRODUCTION

The events related to type 1 diabetes (T1D) pathophysiology in humans are poorly defined. For example, we do not understand the initiating trigger for T1D, how β cell loss proceeds, whether the loss is inevitable or can be abrogated, or the potential for residual β cell recovery. The long-standing view of T1D pathogenesis was that autoimmune β cell destruction resulted in complete loss of pancreatic insulin secretion. The improved sensitivity of C-peptide detection as well as studies using pancreatic specimens have recently led to the realization that many individuals with T1D have insulin-secreting cells, even 50 years after diagnosis (Keenan et al., 2010; Oram et al., 2014). Additionally, little is known about the properties of the glucagon-producing α cells in the T1D pancreas and whether they share the plasticity recently described in mouse models of profound β cell loss (Chera et al., 2014; Thorel et al., 2010). Moreover, it is unclear why T1D α cells have impaired glucagon secretion (Bolli et al., 1983; Gerich et al., 1973; Sherr et al., 2014), which contributes to hypoglycemia susceptibility.

To comprehensively define the functional and molecular properties of T1D islets, we used an approach that allows study of the pancreas and isolated islets from the same organ donor. Our findings show that remnant β cells appeared to maintain several features of regulated insulin secretion. In contrast, glucagon secretion was significantly compromised, and the levels of essential α cell transcription factors and their downstream targets involved in α cell electrical activity were reduced. Moreover, an important β-cell-enriched transcription factor was misexpressed in T1D α cells. These results provide insight into the functional and molecular profile of α cells in T1D.

RESULTS

Procurement of Pancreatic Islets and Tissue from the Same Organ Donor Allows for Multifaceted Phenotypic Analysis of T1D Islets

Our methodology for islet isolation and tissue procurement from the same pancreas allowed coupling of islet functional and

Table 1. Demographic Information and Phenotype of T1D Donors

Donors	Age (Years)	T1D Duration (Years)	Ethnicity/Race	Gender	BMI	Cause of Death	High-risk HLA[a]	AutoAb	C-Peptide (ng/mL)	HbA1C[b]
1	12	3	Caucasian	F	26.6	anoxia	DR3, DQ2	mIAA	0.05	9.8
2	13	5	Caucasian	M	19.1	anoxia	DR4, DQ2, DQ8	IA2A, mIAA	<0.02	NA
3 nPOD case no. 6342	14	2	Caucasian	F	24.3	anoxia	DR4	IA2A, mIAA	0.26	9.2
4	20	7	Caucasian	M	25.5	anoxia	DR4, DQ2, DQ8	IA2A	0.43	NA
5 nPOD case no. 6323	22	6	Caucasian	F	24.7	anoxia	DR3, DR4, DQ2	GADA, IA2A	<0.02	6.6
6	27	17	Caucasian	M	18.5	anoxia	DR4, DQ2, DQ8	ND	<0.02	NA
7	30	20	Caucasian	M	29.8	anoxia	DR4, DQ8	ND	<0.02	NA
8	58	31	Caucasian	M	21.7	anoxia	DR4	NA	NA	8.8

The nature of T1D pancreas, organ scarcity, and logistics of organ procurement and processing precluded us from collecting the entire dataset on each T1D donor. Perifusion, donors nos. 1, 3, 4, and 5; qRT-PCR, donors nos. 1, 4, and 5; islet endocrine cell composition by FACS, donors nos. 1, 4, 5, and 8; histology, donors nos. 1, 2, 5, and 8; islet transplantation, donors nos. 1, 5, and 8; α cell purification and RNA sequencing, donors nos. 3, 6, and 7. AutoAb, autoantibodies; GADA, glutamic acid decarboxylase autoantibody; HbA1C, hemoglobin A1C; IA2A, autoantibody to transmembrane protein of the protein tyrosine phosphatase family; mIAA, insulin autoantibody; NA, not available; ND, non-detectable.

[a]HLA typing provided by Organ Procurement Organization.

[b]HbA1C collected from donor's redacted medical chart.

molecular analysis with histological assessment of islets in the native organ (Figure S1A). In this way, we were able to study 5 donors with recent-onset T1D (<10 years of T1D duration) and 3 donors with long-standing T1D (>10 years of T1D duration) receiving continuous insulin therapy compared to the appropriate non-diabetic controls (Tables 1 and S1). Experimental approaches used for analysis of each T1D donor are indicated in Table 1 and labeled accordingly in figure legends. Due to clinical heterogeneity of T1D, we confirmed disease status by DNA sequencing (Sanyoura et al., 2018) as described in the Supplemental Experimental Procedures. DNA sequencing covering coding regions and splice junctions of 148 genes associated with monogenic diabetes did not detect variants associated with monogenic diabetes (Alkorta-Aranburu et al., 2016; Table S2). By flow cytometry analysis, recent-onset T1D islets contained 7-fold more α cells than β cells, and the β cell fraction was reduced approximately 6-fold compared to normal islets (Blodgett et al., 2015; Figures S1B–S1D).

T1D β Cells Have Regulated Insulin Secretion and Express Key Transcriptional Regulators

Next, we analyzed the secretory function of the T1D islets in a dynamic cell perifusion system and compared it with islets from normal donors (Kayton et al., 2015). We found that the few remaining T1D β cells responded to glucose, cyclic AMP (cAMP)-evoked stimulation, and KCl-mediated depolarization with a similar pattern as controls (Figures 1A and 1B). The biphasic glucose-stimulated insulin secretion in islets at T1D onset was also shown recently by Krogvold and colleagues (Krogvold et al., 2015). As expected, insulin secretion by T1D islets was diminished when normalized to overall islet cell volume (expressed in islet equivalents [IEQs]; Figure 1A) due to the greatly reduced β cell number (Figure S1C). However, insulin secretion normalized to islet insulin content (reflecting β cell number) by T1D islets nearly overlapped in terms of magnitude with the secretory response of controls (Figure 1B). Consistent with flow cytometry data in Figure S1C, the T1D β cell population was 4- to 6-fold less than in control islets when adjusted to islet insulin content (Figure 1C). Furthermore, the expression of transcription factors critical for β cell identity *PDX1* (Gao et al., 2014) and *NKX6.1* (Taylor et al., 2013) was not changed in either isolated T1D islets (Figure 1D) or by protein analysis of the native pancreatic tissue (Figures 1E, 1F, and S2). Even in the 58-year-old T1D donor with long-standing T1D, these transcription factors were expressed in rare insulin+ cells found scattered in the exocrine parenchyma (Figures 1E, 1F, and S2). However, *MAFA* (Guo et al., 2013), a transcription factor known to be required for murine β cell maturation, was reduced in the T1D islet (Figure 1D), and there were fewer NKX2.2-expressing T1D β cells compared to controls (Figures 1G and S2), even though islet *NKX2-2* mRNA was unchanged (Figure 1D). These studies allowed us to directly access multiple pathways of insulin secretion and suggest that the T1D β cells appear to maintain several functional features of normal β cells, supporting the notion that T1D is a disease primarily of β cell loss. Due to very few T1D β cells available for deeper analyses, we focused our efforts on comprehensive characterization of the most abundant endocrine cell type in T1D islets, the α cell (Figure S1C).

T1D α Cells Are Functionally Impaired and Have Altered Expression of Transcription Factors Constituting α and β Cell Identity

Surprisingly, in spite of T1D islets containing 2-fold more α cells than normal islets (Figure S1C), their glucagon secretion was not significantly increased compared to controls when normalized to overall islet cell volume (expressed as IEQs; Figure 2A). The response was reduced when normalized to islet glucagon content (Figures 2B and 2C) and lacked the appropriate increase at low glucose following 30-min high glucose inhibition (Figure 2B, inset). Marchetti and colleagues (Marchetti et al., 2000) observed a similar defect in glucagon secretion in islets isolated from a single T1D donor 8 months after the disease onset. These

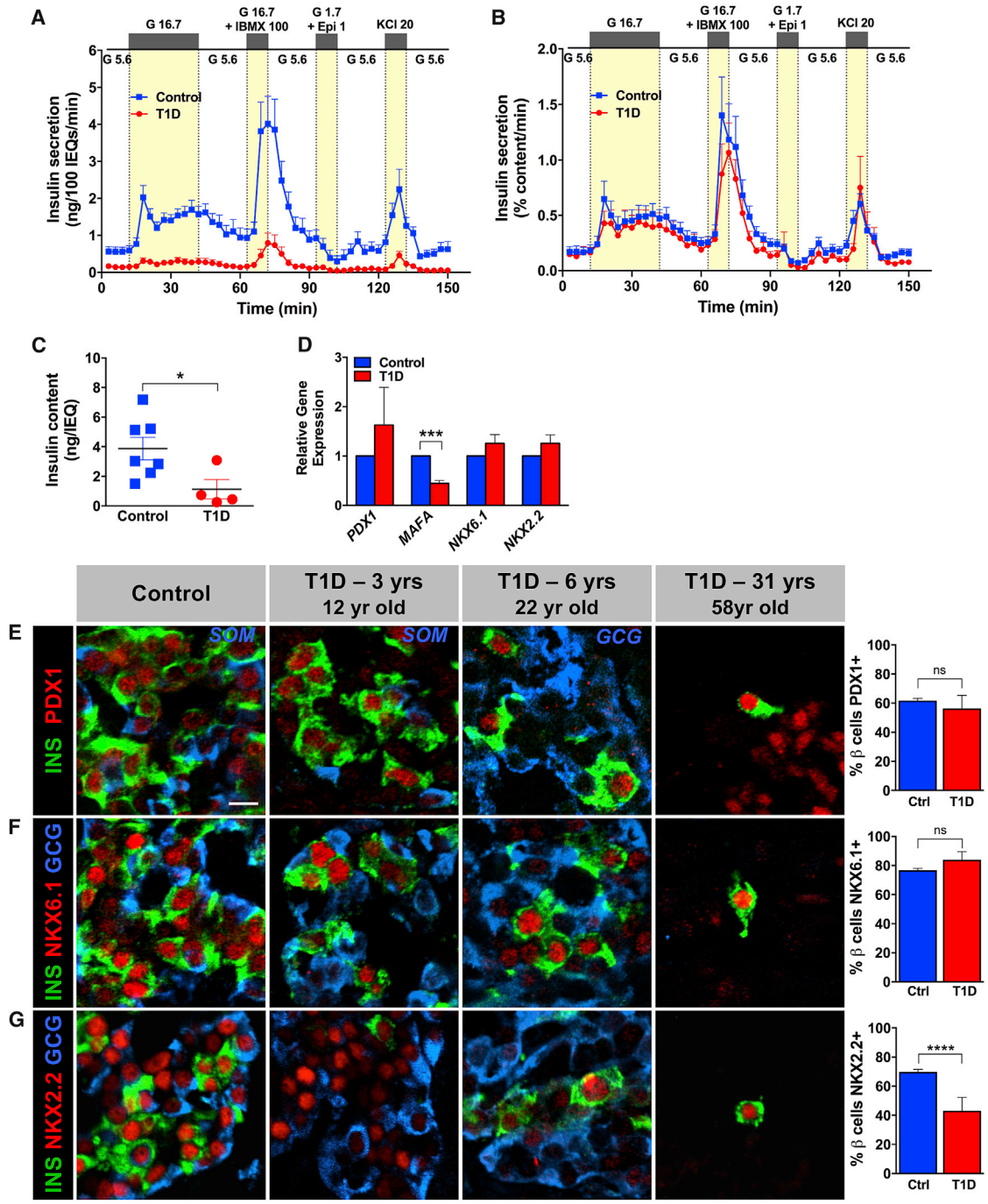

Figure 1. T1D β Cells in Recent-Onset T1D Retain Secretory Properties and Gene Expression Pattern Similar to Normal β Cells

(A and B) Insulin secretion was assessed in islets isolated from donors with recent-onset T1D (n = 4; ages 12–22 years; donors nos. 1, 3, 4, and 5) and compared to normal controls (n = 7; ages 7–21 years); G 5.6–5.6 mM glucose, G 16.7–16.7 mM glucose, G 16.7 + IBMX 100–16.7 mM glucose + 100 μM isobutylmethylxanthine (IBMX), G 1.7 + Epi 1–1.7 mM glucose + 1 μM epinephrine, KCl 20–20 mM potassium chloride.

(A) Insulin secretion normalized to overall islet cell volume (expressed as islet equivalents [IEQs]); ****$p < 0.0001$.

(B) Insulin secretion normalized to islet insulin content; ***$p = 0.0005$. Data in (A) and (B) were compared by two-way ANOVA.

(C) Insulin content of control (3.873 ± 0.763 ng/IEQ) and T1D islets (1.131 ± 0.660 ng/IEQ); $p = 0.0394$; data are represented as mean ± SEM.

(D) Expression of β-cell-enriched transcription factors by qRT-PCR in whole T1D islets (n = 3 donors; ages 12–22 years; donors nos. 1, 4, and 5) and controls (n = 3 donors; ages 11–29 years) was normalized to endogenous control and *INS* expression; ***$p < 0.0007$.

(E–G) Expression of β-cell-enriched transcription factors in the native pancreatic tissue from donors with recent-onset T1D (n = 2; ages 12–22 years; donors nos. 1 and 5) was compared to 58-year-old donor with 31 years of T1D duration (donor no. 8) and controls (n = 7; ages 8–55 years). The pancreas of 58-year-old T1D

(legend continued on next page)

functional changes in T1D α cells were accompanied by reduced mRNA expression of two bona fide α cell regulators *ARX* (Courtney et al., 2013) and *MAFB* (Guo et al., 2013) in isolated islets (Figure 2D). Notably, histological analysis of native tissues further revealed that most α cells from T1D donors did not express MAFB and ARX (Figures 2E, 2F, and S3) but did express low levels of NKX6.1 (Figures 2G and S3), which is normally only found in β cells (Figures 1G and S2). A similar pattern has been seen in a mouse model with extreme β cell loss (Chera et al., 2014; Thorel et al., 2010). To test whether there was evidence of α-to-β cell conversion in the T1D donor pancreas, we searched for, but did not find, islet cells co-expressing insulin and glucagon (data not shown). This observation differs from the recently described α-to-β cell conversion in a mouse model of 99% β cell loss (Chera et al., 2014; Thorel et al., 2010).

Non-autoimmune, Normoglycemic Environment Does Not Promote Conversion of T1D α Cells into β Cells

To determine whether human T1D α cells following extreme β cell loss can give rise to β cells when placed in a normoglycemic, non-autoimmune environment, we transplanted islets from the same T1D donors into immunodeficient *Nod-SCID-IL2Rγ^{null}* (NSG) mice (Brissova et al., 2014; Figure 3A). After one-month engraftment, mice were treated with either PBS or exendin-4 (Dai et al., 2017), a GLP-1 analog reported to promote β cell maturation or proliferation for an additional 1 month. At the end of the treatment, *in vivo* insulin secretion was stimulated by a bolus of high glucose and arginine. Although a species-specific assay readily detected a rise in mouse plasma insulin levels, human insulin was undetectable (data not shown), indicating the absence of functional human β cells in T1D islet grafts. Similar to native tissue, graft immunocytochemistry showed that β cells were very rare and did not detect insulin/glucagon co-expression (Figure 3B; data not shown). Because there were no significant phenotypic differences between PBS- and exendin-4-treated groups, these treatment groups were combined to assess α cell transcription factor expression. After transplantation, the number of α cells expressing ARX in T1D islet grafts was greater (Figure 3D) with a decrease in the number of NKX6.1+ α cells (Figure 3E) compared to α cells in the native T1D pancreas, suggesting that the normoglycemic, non-autoimmune environment allowed for partial recovery of α cell identity marker expression.

Genes Critical to α Cell Identity and Function Are Differentially Expressed between T1D and Control α Cells

T1D and control islet α cells were purified by fluorescence-activated cell sorting (FACS) (Figure S4A). RNA-sequencing analysis (RNA-seq) performed on these cells indicated significant differences in the gene expression profiles (Figures 4A, 4B, and S4B). Ingenuity pathway analysis (IPA) and Gene Ontology (GO) term analysis (Tables S3 and S4; Figures S4C and S4D) identified differences in processes associated with protein synthesis and handling, immune-activated signaling, and cell stress response pathways. Specifically, T1D α cells had increased expression of genes important in the unfolded protein response and formation of tight and adhesive junctions. Conversely, T1D α cells had significantly reduced expression of genes recently identified by single-cell RNA-seq as α cell enriched, such as *KLHL41*, *LOXL4*, and *PTGER3* (Muraro et al., 2016; Segerstolpe et al., 2016; Figure 4C). Our RNA-seq analysis further confirmed dysregulated expression of several islet-enriched transcription factors in T1D α cells, which we initially detected by RT-PCR in whole islets and at a protein level in pancreatic tissues (*MAFB*, *ARX*, and *NKX6-1*; Figures 2D–2G and 4C). Among islet-enriched transcription factors, *RFX6*, which lies upstream of *MAFB*, *ARX*, and *NKX6-1* in endocrine cell differentiation (Piccand et al., 2014; Smith et al., 2010), had the most reduced expression (7.2-fold). In mature mouse and human β cells, *RFX6* directly controls expression of P/Q and L-type voltage-gated calcium channels (*CACNA1A*, *CACNA1C*, and *CACNA1D*) and the KATP channel subunit sulfonylurea receptor 1 (*ABCC8*) (Chandra et al., 2014; Piccand et al., 2014; Figure 4C) that associates with Kir6.x pore-forming subunits (Winkler et al., 2009). T1D α cells also had altered expression of potassium and sodium ion channels, vesicle trafficking proteins, and cAMP signaling molecules, which collectively point to altered T1D α cell electrical activity and impaired glucagon exocytosis (Figure 4D).

DISCUSSION

These results show the utility and advantages of an experimental approach that studies the pancreatic tissue and isolated islets from the same T1D individual and incorporates the *in vitro* and *in vivo* analysis of islets removed from the autoimmune, hyperglycemic environment. This approach also allowed us to directly test multiple pathways of hormone secretion and uncouple effects of decreased β cell mass and β cell dysfunction not possible in clinical studies *in vivo*. We found that the rare β cells in the pancreas present not only in recent-onset T1D but also many years after T1D diagnosis maintained features of regulated insulin secretion and/or produced key transcriptional regulators known to play a critical role in the maintenance of β cell fate and function. In contrast, T1D α cells, while highly abundant, were functionally impaired. Impaired glucagon secretion by T1D islets was associated with altered expression of multiple nuclear regulators (e.g., *ARX*, *MAFB*, and *RFX6*) and their downstream targets, suggesting that these changes directly and indirectly impact glucagon secretory pathways by altering expression of potassium and sodium ion channels, vesicle trafficking proteins, and cAMP signaling molecules. Abnormal glucagon secretion is a common complication of T1D, including impaired counterregulatory response of glucagon to hypoglycemia (Gerich et al., 1973)

donor did not have any insulin+ islets; only rare β cells were found in exocrine parenchyma. T1D β cells (n = 3 donors; ages 12–58 years; donors nos. 1, 5, and 8) had normal expression of β-cell-enriched transcription factors PDX1 (E) and NKX6.1 (F) but decreased expression of NKX2.2 (G) compared to controls (n = 7 donors; ages 8–55 years); ****$p < 0.0001$; ns, not significant.

Data in (C)–(G) were compared by two-tailed Student's t test. Data in (A)–(G) are shown as mean ± SEM. The scale bar in (E) represents 10 μm and also corresponds to (F) and (G). See also Figures S1 and S2.

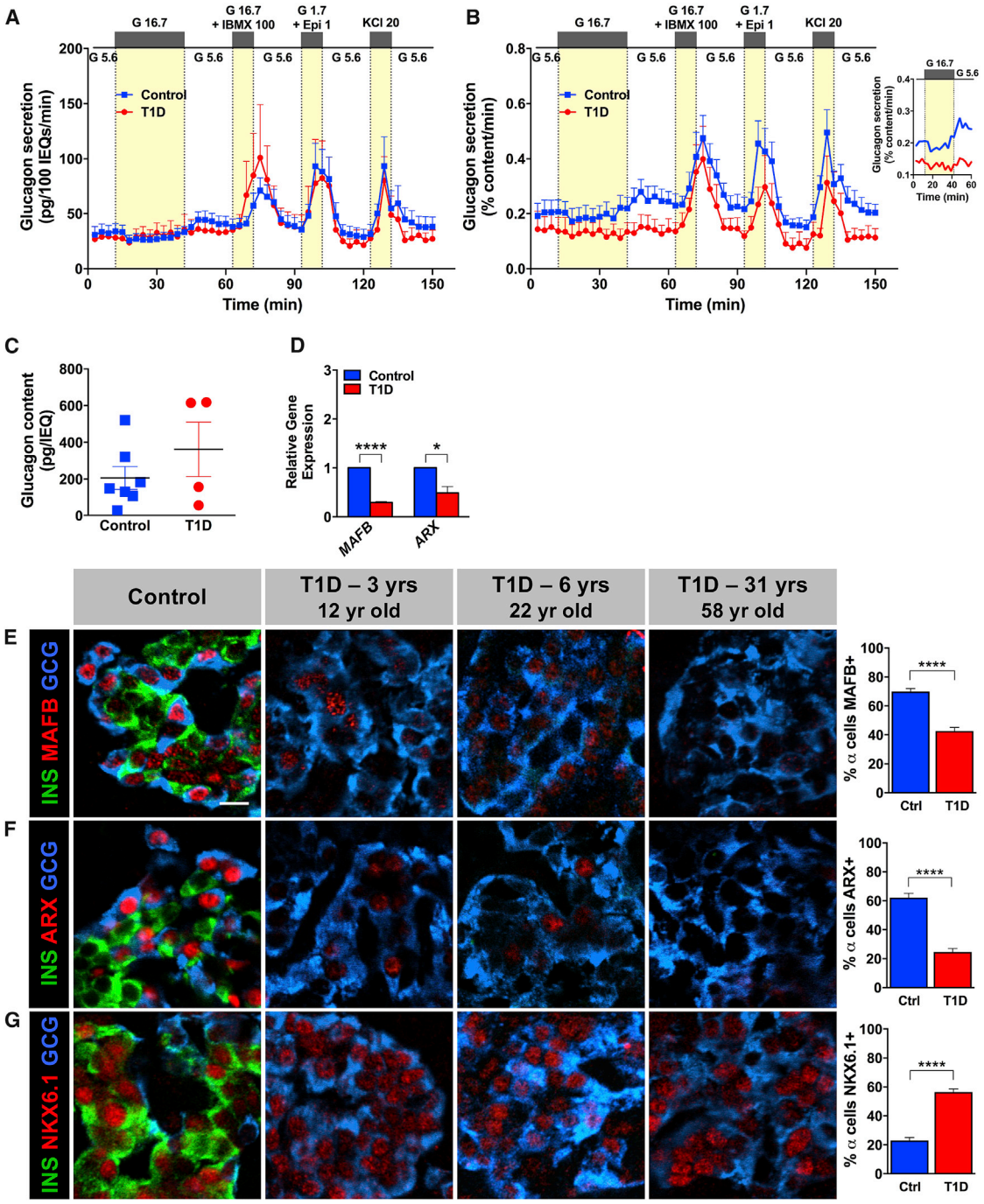

Figure 2. T1D α Cells in Recent-Onset T1D Have Reduced Glucagon Secretion and Dysregulated Gene Expression

The same sets of islets shown in Figures 1A and 1B were simultaneously analyzed for glucagon secretion. The same non-diabetic controls were used as Figure 1. The labeling of islet stimuli is identical to that in Figure 1.

(A) Glucagon secretion normalized to overall islet cell volume (expressed as IEQs); p = 0.2470.

(B) Glucagon secretion normalized to islet glucagon content; ****p < 0.0001. Data in (A) and (B) were compared by two-way ANOVA. Inset shows mean glucagon response to low glucose following the 30-min inhibition with high glucose.

(C) Glucagon content in control (206 ± 62 pg/IEQ) and T1D islets (362 ± 149 pg/IEQ); p = 0.2831; data are represented as mean ± SEM.

(D) Expression of α-cell-enriched factors by qRT-PCR in whole T1D islets (n = 3 donors; ages 12–22 years; donors nos. 1, 4, and 5) and controls (n = 3 donors; ages 11–29 years) was normalized to endogenous control and *GCG* expression; ****p < 0.0001; *p = 0.0184.

(legend continued on next page)

and an inappropriate rise in circulating glucagon in response to a mixed meal challenge (Sherr et al., 2014). Defects in neural glucose sensing, impaired islet innervation, or intra-islet insulin deficiency have been proposed to explain these abnormalities in glucagon secretion (Mundinger et al., 2016). The current analysis provides a new explanation and molecular mechanism for the dysregulated glucagon secretion in T1D, namely an intrinsic α cell defect (Figure 4D). Our observation that the changes in α cell gene expression partially resolved when T1D islets were transplanted into a normoglycemic, non-autoimmune environment suggests that interventions might be developed to improve α cell gene expression and glucagon secretion in T1D.

These data provide insight and raise important questions about the molecular and functional changes in human T1D α cells. After massive β cell loss in mice, β cells can be gradually and partially replenished by a sustained α-to-β cell reprogramming (Chera et al., 2014; Thorel et al., 2010). Unlike in mice, the current analysis did not identify cells co-expressing insulin and glucagon in the native pancreas or after transplantation into a normoglycemic, non-autoimmune environment, further supporting the notion that α-to-β cell conversion in humans is a very rare event (Chakravarthy et al., 2017). Our findings do suggest that T1D α cells have reduced key molecular regulators (*ARX* and *MAFB*) and express a transcription factor, NKX6.1, that is usually β cell specific, raising the possibility of partial change toward a β cell phenotype. Perhaps an additional stimulus or multiple stimuli may be required for human α cell reprogramming. Lineage-tracing studies of human α cells are needed to investigate the plasticity of human α cells.

These results stimulate a number of questions about the molecular and cellular changes in T1D islets. Are the α cell changes the result of the autoimmune attack on the β cells also affecting α cells, the lack of α cell-β cell contact, the diabetic milieu of hyperglycemia, or reduced intra-islet insulin? Have the remnant β cells, which have a number of features of normal β cells, somehow escaped the autoimmunity; do they comprise a specific subset of β cells (Dorrell et al., 2016); or do they represent an incomplete regenerative attempt, arising via *de novo* neogenesis from facultative pancreas progenitors (Xu et al., 2008), β replication (Brissova et al., 2014; Cano et al., 2008; Nir et al., 2007), and/or transdifferentiation of acinar cells (Zhou et al., 2008) or other islet endocrine cell types, such as α cells (Chera et al., 2014; Thorel et al., 2010)? Additional studies of isolated T1D islets and T1D pancreatic tissue are needed to better understand the phenotype and possible heterogeneity of T1D α and β cells.

EXPERIMENTAL PROCEDURES

Further details and an outline of resources used in this work can be found in Supplemental Experimental Procedures (Resources Table).

Animals

Immunodeficient 10- to 12-week-old NSG male mice were used for human islet transplantation studies (Brissova et al., 2014; Dai et al., 2016). Animals were maintained by Vanderbilt Division of Animal Care in group housing in sterile containers within a pathogen-free barrier facility housed with a 12 hr light/12 hr dark cycle and access to free water and standard rodent chow. All animal procedures were approved from by the Vanderbilt Institutional Animal Care and Use Committees.

Primary Cell Cultures

Primary human islets were cultured in CMRL 1066 media (5.5 mM glucose, 10% FBS, 1% Pen/Strep, and 2 mM L-glutamine) in 5% CO_2 at 37°C for 24–72 hr prior to reported studies (Brissova et al., 2014; Dai et al., 2016). No cell lines were used in this study.

Human Subjects

Pancreata and islets from normal and T1D donors were obtained through a partnership with the International Institute for Advancement of Medicine (IIAM), National Disease Research Interchange (NDRI), Integrated Islet Distribution Program (IIDP), and Network for Pancreatic Organ Donors with Diabetes (nPOD). Most pancreata from normal donors were processed either for islet isolation (Balamurugan et al., 2003) or histological analysis (described below and Table S1). In most T1D pancreatic organs, islets and tissue specimens were procured from the same organ. For a number of controls, human islets were obtained through IIDP (Table S1). Donor demographic information and phenotype of T1D donors is summarized in Table 1. The Vanderbilt University Institutional Review Board declared studies on de-identified human pancreatic specimens do not qualify as human subject research.

Human Pancreatic Islet Procurement

Pancreata from normal juvenile and T1D donors were received within 18 hr from cold clamp and maintained in cold preservation solution on ice until processing. Pancreas was then cleaned from connective tissue and fat, measured, and weighed. Prior to islet isolation, multiple cross-sectional slices of pancreas with 2- to 3-mm thickness were obtained from the head, body, and distal tail (Figure S1A). Pancreatic slices were further divided into four quadrants and then either snap frozen or processed for cryosections. Tissue specimens processed for cryosections were fixed in 0.1 M PBS containing 4% paraformaldehyde (Electron Microscopy Sciences) for 3 hr on ice with mild agitation, washed in four changes of 0.1 M PBS over 2 hr, equilibrated in 30% sucrose/0.01 M PBS overnight, and embedded in Tissue-Plus O.C.T. compound (Fisher Scientific). Pancreatic organs were processed for islet isolation using an approach previously described (Balamurugan et al., 2003). Briefly, depending on the size of pancreatic duct, 18G or 22G catheters were inserted into the main pancreatic duct (one catheter toward head and the other one toward tail). Accessory duct and main pancreatic duct were clamped at the points where sections were collected to prevent leakage of collagenase solution during infusion. Collagenase solution consisting of collagenase NB1 (1,600 U/isolation; Crescent Chemical), neutral protease NB1 (200 U/isolation; Crescent Chemical), and DNase I (12,000 U/isolation; Worthington Biochemical Corporation) was pre-warmed to 28°C and delivered intraductally using a Rajotte's perfusion system and then maintained at 37°C for approximately 20 min. The inflated tissue was then transferred to a Ricordi's chamber apparatus for combined mechanical and enzymatic digestion, which was maintained at 36°C for 5–15 min prior to warm and cold collection. The digest was incubated in cold RPMI media (Mediatech) supplemented with heat-inactivated 10% fetal calf serum (Life Technologies) for 1 hr on ice.

(E–G) Analysis of native pancreatic tissue for expression of islet-enriched transcription factors. T1D α cells (n = 4 donors; ages 12–58 years; donors nos. 1, 2, 5, and 8) expressed β cell marker NKX6.1 (G) and lost bona fide α cell markers MAFB (E) and ARX (F) in most T1D α cells compared to controls (n = 7 donors; ages 8–55 years); ****$p < 0.0001$.

Data in (C)–(G) were compared by two-tailed Student's t test. Data in (A)–(G) are shown as mean ± SEM. The scale bar in (E) represents 10 μm and also corresponds to (F) and (G). See also Figures S1 and S3.

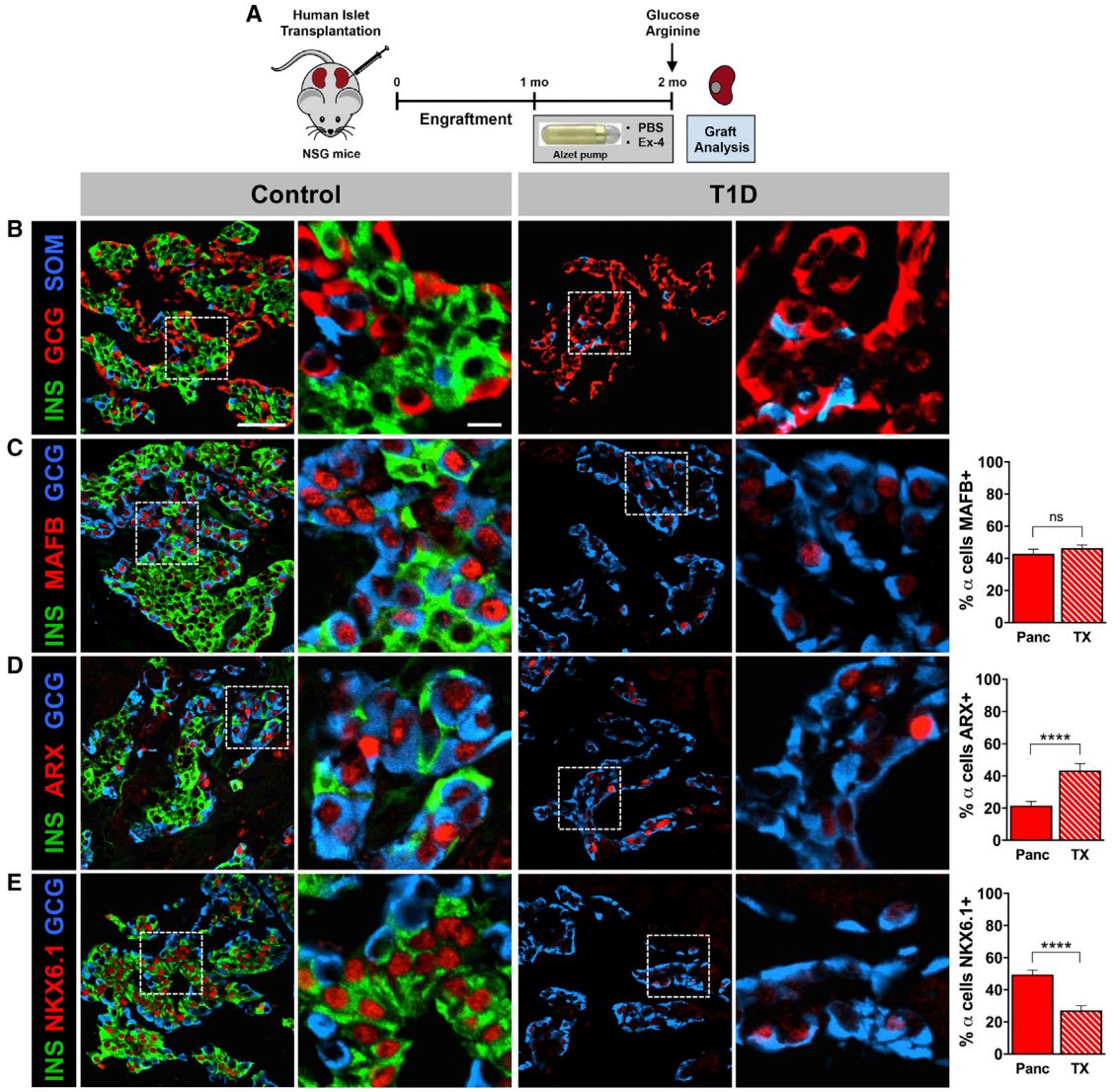

Figure 3. T1D α Cells Do Not Show Evidence of α-to-β Cell Reprogramming in Normoglycemic, Non-autoimmune Environment

(A) Islets from donors with recent-onset and long-standing T1D (n = 3 donors; 12–58 years; donors nos. 1, 5, and 8) depicted in Figures 1 and 2 were transplanted into NSG mice. After 1-month engraftment, mice were treated with either PBS or Ex-4 for an additional 1 month. Representative images of islet grafts are from the 12-year-old individual with 3-year T1D duration (donor no. 1). In control and T1D columns, regions denoted by the dashed line in images on the left (B)–(E) (scale bar in B is 50 μm) are displayed on the right (scale bar is 10 μm).

(B) Insulin (INS) and glucagon (GCG) double-positive cells were not detected in either type of T1D islet grafts (PBS or Ex-4).

(C–E) As there were no phenotypic differences between PBS and Ex-4 treatment groups, representative images were taken from both cohorts and analyzed for α cell transcription factor expression. Change in number of GCG+ cells expressing MAFB (C), ARX (D), and NKX6.1 (E) in transplanted T1D islets (TX) relative to donor's native pancreas (Panc) is shown. ****$p < 0.0001$; ns, not significant.

Data in (C)–(E) are shown as mean ± SEM and were compared by two-tailed Student's t test.

If post-digestion tissue pellet was larger than 2 mL and islets were distinguishable from exocrine tissue by Dithizone staining (Sigma), a purification step consisting of density gradient (Biocoll; Cedarlane) centrifugation on a COBE 2991 Cell Processor (Gambro-Terumo) was used to separate islets from exocrine tissue. Islets were re-suspended in CMRL 1066 medium (Mediatech) supplemented with 10% heat-inactivated fetal calf serum (Life Technologies), 100 units/mL penicillin/0.1 mg/mL streptomycin (Life Technologies), and 2 mmol/L L-glutamine (Life Technologies). On average, islet-enriched fraction contained from 30,000 (T1D pancreas) to 90,000 IEQs (normal pancreas) with 25%–50% purity. Islets were cultured for 12–24 hr and then shipped from Pittsburgh to Vanderbilt University and/or University of Massachusetts for further analysis following shipping protocols developed by the Integrated Islet Distribution Program (IIDP). Subsequent assays with isolated islets were set up within 24–48 hr of islet arrival.

Statistical Analysis

To compare global differences in perifusion outcomes in T1D donors and controls, two-way ANOVA with Sidak's multiple comparisons test was used. Data were expressed as mean ± SEM. Two-tailed Student's t test was used for

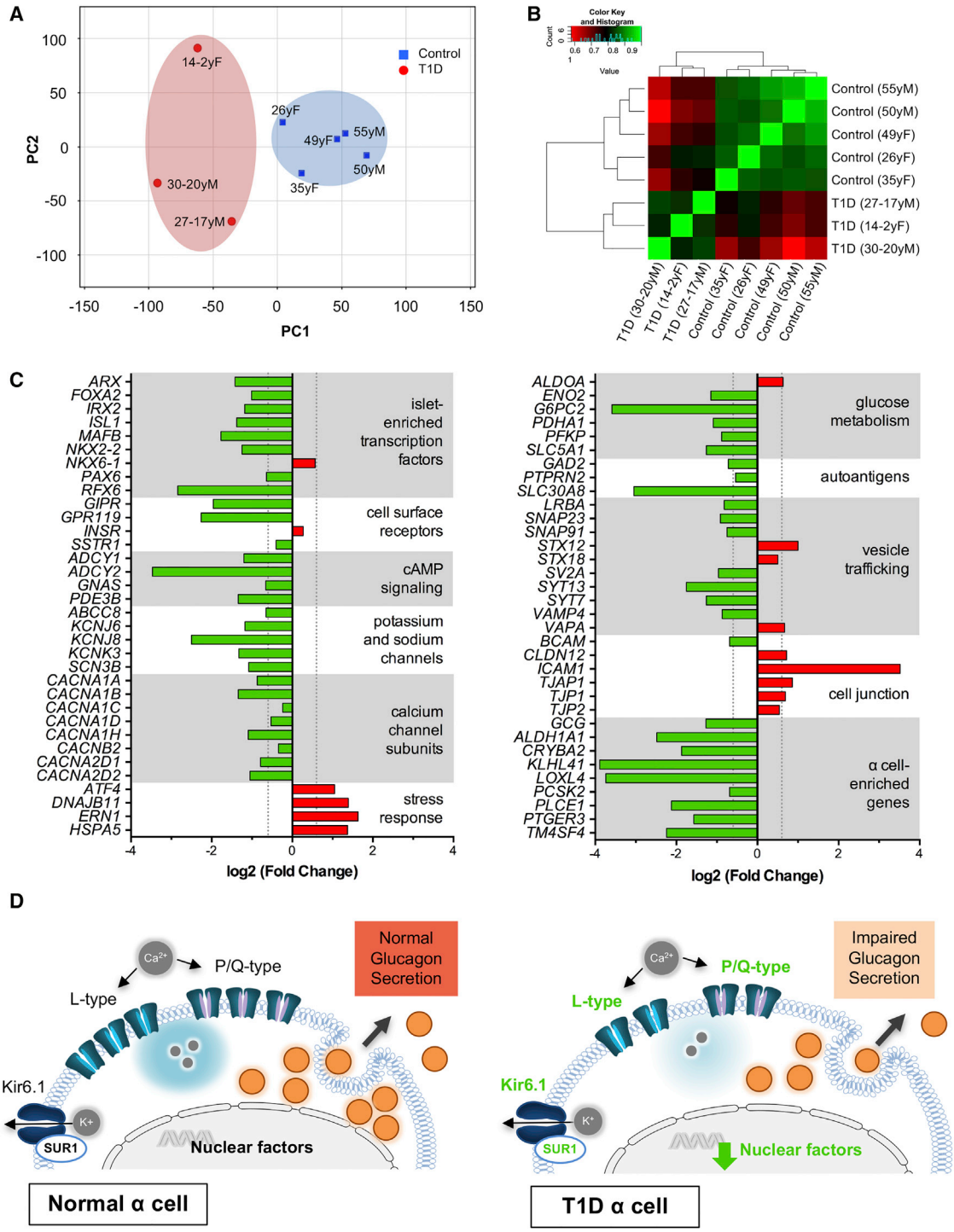

Figure 4. Genes Critical to α Cell Function Are Differentially Expressed in T1D α Cells

Transcriptome by RNA-sequencing analysis of purified human α cells from T1D donors (n = 3; ages 14–30 years; donors nos. 3, 6, and 7) and controls (n = 5; ages 26–55 years).

(A) Principal-component analysis (PCA) plot shows clustering of α cell samples from control and T1D donors.

(B) Heatmap of the pairwise correlation between all samples based on the Spearman correlation coefficient. Perfect correlation is indicated by 1.

(C) Genes associated with α cell identity and function are significantly downregulated in the T1D α cells with increased expression of stress response factors and cell-cell contact proteins. Vertical dotted lines represent point of significance for fold change (FC) = 1.5× threshold analysis; $p < 0.05$ for all values shown.

(legend continued on next page)

analysis of statistical significance for two-group comparisons between T1D donors and controls. A p value less than 0.05 was considered significant. Statistical analysis was performed using GraphPad Prism software. Statistical details of experiments are described in the figure legends, Results section, and Supplemental Experimental Procedures.

DATA AND SOFTWARE AVAILABILITY

The accession number for the sequencing data reported in this paper is GEO: GSE106148.

SUPPLEMENTAL INFORMATION

Supplemental information includes Supplemental Experimental Procedures, four figures, and four tables and can be found with this article online at https://doi.org/10.1016/j.celrep.2018.02.032.

ACKNOWLEDGMENTS

We thank Dr. Seung Kim for providing critical comments on the manuscript. We are very grateful to Drs. Raphael Scharfmann, Michael German, and Gérard Gradwohl for helpful discussions and sharing reagents. Special thanks to Mr. David Scheel for experimental advice. This research was performed using resources and/or funding provided by the NIDDK-supported Human Islet Research Network (HIRN, RRID:SCR_014393; https://hirnetwork.org; UC4 DK104211, DK108120, and DK112232), by DK106755, DK72473, DK89572, DK97829, DK94199, the Vanderbilt Diabetes Research and Training Center (DK20593), and by grants from the JDRF (2-SRA-2015-68-Q-R, 2-SRA-2016-149-Q-R, 17-2013-321, 17-2013-324), the Leona M. and Harry B. Helmsley Charitable Trust, and the Department of Veterans Affairs (BX000666). Islet imaging and functional analysis were performed with the support of the Cell Imaging Shared Resource and Islet Procurement and Analysis Core of the Vanderbilt Diabetes Research and Training Center (DK20593). Flow cytometry analysis was performed in the Vanderbilt Flow Cytometry Shared Resource (P30 CA68485 and DK058404). C-peptide and autoantibodies were analyzed at the Northwest Lipid Metabolism and Diabetes Research Laboratories and Barbara Davis Center for Childhood Diabetes, respectively. This research was performed with the support of the Network for Pancreatic Organ Donors with Diabetes (nPOD; www.jdrfnpod.org) and the Integrated Islet Distribution Program (IIDP; https://iidp.coh.org/). We are grateful to Organ Procurement Organizations partnering with the International Institute for Advancement of Medicine and National Disease Research Interchange. We are especially thankful to organ donors and their families.

AUTHOR CONTRIBUTIONS

Conceived and Designed the Experiments, M.B., R.H., D.S., S.S., N.P., R.B., M.C.-T., M.A., D.M.H., R.S., and A.C.P.; Conducted the Experiments, M.B., R.H., D.S., S.S., N.P., C.D., D.M.B., R.B., R.A., G.P., J.L., F.C.P., and M.S.; Analyzed and Interpreted the Data, M.B., R.H., D.S., S.S., C.D., D.M.B., R.B., R.A., G.P., M.S., L.H.P., D.M.H., R.S., S.E.L., and A.C.P.; Wrote the Manuscript, M.B., R.H., D.S., S.S., and A.C.P.; Reviewed/Edited the Manuscript, M.B., R.H., D.S., S.S., C.D., D.M.B., R.B., M.C.-T., R.A., G.P., J.L., F.C.P., M.G.v.H., D.L.G., L.D.S., M.S., L.H.P., M.A., D.M.H., S.E.L., N.P., R.S., and A.C.P.

DECLARATION OF INTERESTS

M.G.v.H. is an employee of Novo Nordisk.

Received: December 28, 2017
Revised: January 2, 2018
Accepted: February 8, 2018
Published: March 6, 2018

REFERENCES

Alkorta-Aranburu, G., Sukhanova, M., Carmody, D., Hoffman, T., Wysinger, L., Keller-Ramey, J., Li, Z., Johnson, A.K., Kobiernicki, F., Botes, S., et al. (2016). Improved molecular diagnosis of patients with neonatal diabetes using a combined next-generation sequencing and MS-MLPA approach. J. Pediatr. Endocrinol. Metab. *29*, 523–531.

Balamurugan, A.N., Chang, Y., Fung, J.J., Trucco, M., and Bottino, R. (2003). Flexible management of enzymatic digestion improves human islet isolation outcome from sub-optimal donor pancreata. Am. J. Transplant. *3*, 1135–1142.

Blodgett, D.M., Nowosielska, A., Afik, S., Pechhold, S., Cura, A.J., Kennedy, N.J., Kim, S., Kucukural, A., Davis, R.J., Kent, S.C., et al. (2015). Novel observations from next-generation RNA sequencing of highly purified human adult and fetal islet cell subsets. Diabetes *64*, 3172–3181.

Bolli, G., de Feo, P., Compagnucci, P., Cartechini, M.G., Angeletti, G., Santeusanio, F., Brunetti, P., and Gerich, J.E. (1983). Abnormal glucose counterregulation in insulin-dependent diabetes mellitus. Interaction of anti-insulin antibodies and impaired glucagon and epinephrine secretion. Diabetes *32*, 134–141.

Brissova, M., Aamodt, K., Brahmachary, P., Prasad, N., Hong, J.-Y., Dai, C., Mellati, M., Shostak, A., Poffenberger, G., Aramandla, R., et al. (2014). Islet microenvironment, modulated by vascular endothelial growth factor-A signaling, promotes β cell regeneration. Cell Metab. *19*, 498–511.

Cano, D.A., Rulifson, I.C., Heiser, P.W., Swigart, L.B., Pelengaris, S., German, M., Evan, G.I., Bluestone, J.A., and Hebrok, M. (2008). Regulated beta-cell regeneration in the adult mouse pancreas. Diabetes *57*, 958–966.

Chakravarthy, H., Gu, X., Enge, M., Dai, X., Wang, Y., Damond, N., Downie, C., Liu, K., Wang, J., Xing, Y., et al. (2017). Converting adult pancreatic islet α cells into β cells by targeting both Dnmt1 and Arx. Cell Metab. *25*, 622–634.

Chandra, V., Albagli-Curiel, O., Hastoy, B., Piccand, J., Randriamampita, C., Vaillant, E., Cavé, H., Busiah, K., Froguel, P., Vaxillaire, M., et al. (2014). RFX6 regulates insulin secretion by modulating Ca2+ homeostasis in human β cells. Cell Rep. *9*, 2206–2218.

Chera, S., Baronnier, D., Ghila, L., Cigliola, V., Jensen, J.N., Gu, G., Furuyama, K., Thorel, F., Gribble, F.M., Reimann, F., and Herrera, P.L. (2014). Diabetes recovery by age-dependent conversion of pancreatic δ-cells into insulin producers. Nature *514*, 503–507.

Courtney, M., Gjernes, E., Druelle, N., Ravaud, C., Vieira, A., Ben-Othman, N., Pfeifer, A., Avolio, F., Leuckx, G., Lacas-Gervais, S., et al. (2013). The inactivation of Arx in pancreatic α-cells triggers their neogenesis and conversion into functional β-like cells. PLoS Genet. *9*, e1003934.

Dai, C., Kayton, N.S., Shostak, A., Poffenberger, G., Cyphert, H.A., Aramandla, R., Thompson, C., Papagiannis, I.G., Emfinger, C., Shiota, M., et al. (2016). Stress-impaired transcription factor expression and insulin secretion in transplanted human islets. J. Clin. Invest. *126*, 1857–1870.

Dai, C., Hang, Y., Shostak, A., Poffenberger, G., Hart, N., Prasad, N., Phillips, N., Levy, S.E., Greiner, D.L., Shultz, L.D., et al. (2017). Age-dependent human β cell proliferation induced by glucagon-like peptide 1 and calcineurin signaling. J. Clin. Invest. *127*, 3835–3844.

Dorrell, C., Schug, J., Canaday, P.S., Russ, H.A., Tarlow, B.D., Grompe, M.T., Horton, T., Hebrok, M., Streeter, P.R., Kaestner, K.H., and Grompe, M. (2016). Human islets contain four distinct subtypes of β cells. Nat. Commun. *7*, 11756.

(D) Proposed model for disrupted glucagon secretion in T1D α cells. Normal α cell function is maintained by islet-enriched transcription factors, which regulate α cell machinery necessary for glucagon synthesis and secretion (left panel). Altered expression of transcription factors likely leads to reduced α cell glucagon production, disrupted calcium signaling, and electrical activity that results in impaired glucagon secretion (right panel; green font indicates downregulation). See also data in Figure S4 and Tables S3 and S4.

Gao, T., McKenna, B., Li, C., Reichert, M., Nguyen, J., Singh, T., Yang, C., Pannikar, A., Doliba, N., Zhang, T., et al. (2014). Pdx1 maintains β cell identity and function by repressing an α cell program. Cell Metab. *19*, 259–271.

Gerich, J.E., Langlois, M., Noacco, C., Karam, J.H., and Forsham, P.H. (1973). Lack of glucagon response to hypoglycemia in diabetes: evidence for an intrinsic pancreatic alpha cell defect. Science *182*, 171–173.

Guo, S., Dai, C., Guo, M., Taylor, B., Harmon, J.S., Sander, M., Robertson, R.P., Powers, A.C., and Stein, R. (2013). Inactivation of specific β cell transcription factors in type 2 diabetes. J. Clin. Invest. *123*, 3305–3316.

Kayton, N.S., Poffenberger, G., Henske, J., Dai, C., Thompson, C., Aramandla, R., Shostak, A., Nicholson, W., Brissova, M., Bush, W.S., and Powers, A.C. (2015). Human islet preparations distributed for research exhibit a variety of insulin-secretory profiles. Am. J. Physiol. Endocrinol. Metab. *308*, E592–E602.

Keenan, H.A., Sun, J.K., Levine, J., Doria, A., Aiello, L.P., Eisenbarth, G., Bonner-Weir, S., and King, G.L. (2010). Residual insulin production and pancreatic ß-cell turnover after 50 years of diabetes: Joslin Medalist Study. Diabetes *59*, 2846–2853.

Krogvold, L., Skog, O., Sundström, G., Edwin, B., Buanes, T., Hanssen, K.F., Ludvigsson, J., Grabherr, M., Korsgren, O., and Dahl-Jørgensen, K. (2015). Function of isolated pancreatic islets from patients at onset of type 1 diabetes: insulin secretion can be restored after some days in a nondiabetogenic environment in vitro: results from the DiViD study. Diabetes *64*, 2506–2512.

Marchetti, P., Dotta, F., Ling, Z., Lupi, R., Del Guerra, S., Santangelo, C., Realacci, M., Marselli, L., Di Mario, U., and Navalesi, R. (2000). Function of pancreatic islets isolated from a type 1 diabetic patient. Diabetes Care *23*, 701–703.

Mundinger, T.O., Mei, Q., Foulis, A.K., Fligner, C.L., Hull, R.L., and Taborsky, G.J., Jr. (2016). Human type 1 diabetes is characterized by an early, marked, sustained, and islet-selective loss of sympathetic nerves. Diabetes *65*, 2322–2330.

Muraro, M.J., Dharmadhikari, G., Grün, D., Groen, N., Dielen, T., Jansen, E., van Gurp, L., Engelse, M.A., Carlotti, F., de Koning, E.J.P., and van Oudenaarden, A. (2016). A single-cell transcriptome atlas of the human pancreas. Cell Syst. *3*, 385–394.e3.

Nir, T., Melton, D.A., and Dor, Y. (2007). Recovery from diabetes in mice by beta cell regeneration. J. Clin. Invest. *117*, 2553–2561.

Oram, R.A., Jones, A.G., Besser, R.E.J., Knight, B.A., Shields, B.M., Brown, R.J., Hattersley, A.T., and McDonald, T.J. (2014). The majority of patients with long-duration type 1 diabetes are insulin microsecretors and have functioning beta cells. Diabetologia *57*, 187–191.

Piccand, J., Strasser, P., Hodson, D.J., Meunier, A., Ye, T., Keime, C., Birling, M.-C., Rutter, G.A., and Gradwohl, G. (2014). Rfx6 maintains the functional identity of adult pancreatic β cells. Cell Rep. *9*, 2219–2232.

Sanyoura, M., Jacobsen, L., Carmody, D., Del Gaudio, D., Alkorta-Aranburu, G., Arndt, K., Hu, Y., Kobiernicki, F., Kusmartseva, I., Atkinson, M.A., et al. (2018). Pancreatic histopathology of human monogenic diabetes due to causal variants in KCNJ11, HNF1A, GATA6, and LMNA. J. Clin. Endocrinol. Metab. *103*, 35–45.

Segerstolpe, Å., Palasantza, A., Eliasson, P., Andersson, E.-M., Andréasson, A.-C., Sun, X., Picelli, S., Sabirsh, A., Clausen, M., Bjursell, M.K., et al. (2016). Single-cell transcriptome profiling of human pancreatic islets in health and type 2 diabetes. Cell Metab. *24*, 593–607.

Sherr, J., Tsalikian, E., Fox, L., Buckingham, B., Weinzimer, S., Tamborlane, W.V., White, N.H., Arbelaez, A.M., Kollman, C., Ruedy, K.J., et al. (2014). Evolution of abnormal plasma glucagon responses to mixed-meal feedings in youth with type 1 diabetes during the first 2 years after diagnosis. Diabetes Care *37*, 1741–1744.

Smith, S.B., Qu, H.-Q., Taleb, N., Kishimoto, N.Y., Scheel, D.W., Lu, Y., Patch, A.-M., Grabs, R., Wang, J., Lynn, F.C., et al. (2010). Rfx6 directs islet formation and insulin production in mice and humans. Nature *463*, 775–780.

Taylor, B.L., Liu, F.-F., and Sander, M. (2013). Nkx6.1 is essential for maintaining the functional state of pancreatic beta cells. Cell Rep. *4*, 1262–1275.

Thorel, F., Népote, V., Avril, I., Kohno, K., Desgraz, R., Chera, S., and Herrera, P.L. (2010). Conversion of adult pancreatic α-cells to β-cells after extreme β-cell loss. Nature *464*, 1149–1154.

Winkler, M., Lutz, R., Russ, U., Quast, U., and Bryan, J. (2009). Analysis of two KCNJ11 neonatal diabetes mutations, V59G and V59A, and the analogous KCNJ8 I60G substitution: differences between the channel subtypes formed with SUR1. J. Biol. Chem. *284*, 6752–6762.

Xu, X., D'Hoker, J., Stangé, G., Bonné, S., De Leu, N., Xiao, X., Van de Casteele, M., Mellitzer, G., Ling, Z., Pipeleers, D., et al. (2008). Beta cells can be generated from endogenous progenitors in injured adult mouse pancreas. Cell *132*, 197–207.

Zhou, Q., Brown, J., Kanarek, A., Rajagopal, J., and Melton, D.A. (2008). In vivo reprogramming of adult pancreatic exocrine cells to beta-cells. Nature *455*, 627–632.

Cell Reports, Volume *22*

Supplemental Information

α Cell Function and Gene Expression Are Compromised in Type 1 Diabetes

Marcela Brissova, Rachana Haliyur, Diane Saunders, Shristi Shrestha, Chunhua Dai, David M. Blodgett, Rita Bottino, Martha Campbell-Thompson, Radhika Aramandla, Gregory Poffenberger, Jill Lindner, Fong Cheng Pan, Matthias G. von Herrath, Dale L. Greiner, Leonard D. Shultz, May Sanyoura, Louis H. Philipson, Mark Atkinson, David M. Harlan, Shawn E. Levy, Nripesh Prasad, Roland Stein, and Alvin C. Powers

SUPPLEMENTAL EXPERIMENTAL PROCEDURES

Contact for reagent and resource sharing

Further information and requests for resources and reagents should be directed to and will be fulfilled by the lead contact, Marcela Brissova (marcela.brissova@vanderbilt.edu) or Alvin Powers (al.powers@vanderbilt.edu).

DNA sequencing

DNA samples were sequenced using a custom designed next-generation sequencing (NGS) targeted panel that includes 148 genes implicated in monogenic forms of diabetes (neonatal diabetes and MODY), insulin resistance, lipodystrophy, obesity, rare syndromic forms of diabetes, and diabetes candidate genes (Alkorta-Aranburu et al., 2016). The targeted NGS approach was based on the SureSelect enrichment (Agilent Technologies) protocol followed by MiSeq Illumina NGS. Data quality was assessed using FastQC. Variants were called using The Genome Analysis Toolkit (GATK) HaploTypeCaller v3.3 and assigned to the transcripts of interest. Variants were then annotated in regards to their positions in transcripts of interest, position relative to the coding sequence, consequence for the protein or mRNA and a collection of direct and indirect evidentiary tools and databases including NCBI dbSNP, 1000 Genomes Project, Exome Sequencing Project (ESP), GERP, Conseq, PolyPhen-2, SIFT and the Human Gene Mutation Database (HGMD). All variants were interpreted according to the guidelines of the American College of Medical Genetics. All likely pathogenic variants identified by NGS were confirmed by Sanger sequencing.

Measurement of endocrine cell populations

Islet dissociation and intracellular antibody staining used a previously described protocol (Blodgett et al., 2015). Anti-insulin (Gallus Immunotech), anti-chicken allophycocyanin, (Jackson ImmunoResearch), anti-glucagon (Sigma-Aldrich) conjugated with Zenon Pacific Blue (Invitrogen), and anti-somatostatin (LSBio) conjugated with Zenon Alexa Fluor 488 (Invitrogen) were used to stain β, α, and δ cells, respectively (**Resources Table**). Dissociated islet cell preparations were analyzed using a BD Biosciences FACS Aria II Cell Sorter (University of Massachusetts Medical School Flow Core Laboratory). Cellular debris was eliminated from islet preparations using a forward scatter versus side scatter size gate.

Assessment of pancreatic islet function *in vitro*

Function of islets from T1D donors and normal controls (**Tables 1** and **S1**) was studied in a dynamic cell perifusion system at a perifusate flow rate of 1 mL/min (Kayton et al., 2015). The effluent was collected at 3-minute intervals using an automatic fraction collector. Insulin and glucagon concentrations in each perifusion fraction and islet extracts were measured by radioimmunoassay (Millipore).

qRT-PCR of isolated pancreatic islets

Quantitative reverse transcription polymerase chain reaction (qRT-PCR) was performed using the primer-probe approach from Applied Biosystems (Life Technologies) with *18S* and *ACTB* endogenous controls using Minimum Information for Publication of Quantitative Real-Time PCR Experiments (MIQE) guidelines as described (Brissova et al., 2014). All primers are listed in **Resources Table**. Gene expression in recent-onset T1D donors was compared to normal controls (**Tables 1** and **S1**). We were able to detect *INS* mRNA in T1D islets by RT-PCR and found that it was reduced to 19±7% compared to controls.

α cell sorting by flow cytometry for RNA-sequencing
Human islets were dispersed using a modified protocol as described previously (Aamodt et al., 2016). Briefly, 0.025% trypsin was used to disperse cells and reaction was quenched with modified RPMI medium (10% FBS, 1% Penn/Strep, 5 mM glucose). Cells were washed in the same medium and counted on a hemocytometer, then transferred to FACS buffer (2 mM EDTA, 2% FBS, 1X PBS). Indirect antibody labeling was completed via two sequential incubation periods at 4C, with one wash in FACS buffer following each incubation. Primary and secondary antibodies, listed in **Resources Table**, have been characterized previously and used to isolate high-quality RNA from α cells (Dorrell et al., 2016). Appropriate single color compensation controls were run alongside samples. Prior to sorting, propidium iodide (0.05 ug/100,000 cells; BD Biosciences, San Jose, CA) was added to samples for non-viable cell exclusion. Flow analysis was performed using an LSRFortessa cell analyzer (BD Biosciences), and a FACSAria III cell sorter (BD Biosciences) was used for FACS. Analysis of flow cytometry data was completed using FlowJo 10.1.5 (Tree Star).

Islet transplantation and assessment of grafts
T1D islets were transplanted into immunodeficient 10-12 week old NOD-*scid*-*IL2rγ*^{null} (NSG) male mice. Human islets from three normal donors with an average age of 37 years (range from 20 to 53 years) and average BMI of 25.1 (range from 21.7 to 28.2) were obtained through IIDP (**Table S1**). NSG mice were transplanted beneath the renal capsule with 500 – 600 normal or T1D islet equivalents (prepared as described above). Each set of islets was transplanted into 7-8 mice. Islets were allowed to engraft for 1 month and then mice were randomized for an additional 1-month treatment with either phosphate buffered saline (PBS) or exendin-4 (Ex), which were administered using an Alzet minipump (model 1004 with a pump volume of 100 μL, Durect Corporation). Ex-4 (California Peptide) was reconstituted in PBS without Ca^{2+} and Mg^{2+} and loaded into Alzet pump at concentration of 0.9 mg/mL. Ex-4 in plasma was measured by EIA (Phoenix Pharmaceuticals) and reached concentration of 4.4 ± 0.2 ng/mL (n=8 mice). Insulin secretion in transplanted human islets was assessed by intraperitoneal administration of glucose (2 g/kg of body weight) and arginine (2 g/kg of body weight) prior to and after Ex-4/PBS treatment. Human insulin in plasma was measured by species-specific radioimmunoassay (Millipore).

Immunohistochemical analysis
Immunohistochemical analysis of pancreas was performed on serial 5-μm cryosections from multiple blocks from head, body and tail regions as described (Brissova et al., 2014). Kidneys bearing islet transplants were collected and then 5-μm cryosections from 5-6 different depths of each graft were labeled for immunofluorescence as described (Brissova et al., 2014). Primary antibodies to all antigens and their working dilutions are listed in the **Resources Table**. The antigens were visualized using appropriate secondary antibodies listed in the **Resources Table**. Tyramide Signal Amplification (Perkin Elmer) was used to visualize ARX and NKX2.2 labeling. Digital images were acquired with a Zeiss LSM510 META laser scanning confocal microscope (Carl Zeiss).

RNA-sequencing
Sorted α cells (5,000-125,000) were added to 200 μL lysis/binding solution in the RNAqueous micro-scale phenol-free total RNA isolation kit (Ambion). Trace DNA was removed with TURBO DNA-free (Ambion), RNA integrity was evaluated (Agilent 2100 Bioanalyzer; control, 8.36±0.22 RIN, n=5 donors; T1D, 7.97±0.32 RIN, n=3 donors), and high-integrity total RNA was amplified (Ovation system; NuGen Technologies) per standard protocol as described previously (Brissova et al., 2014). Amplified cDNA was sheared to target 200bp fragment size and libraries were

prepared using NEBNext DNA Library Prep (New England BioLabs). 50bp Paired End (PE) sequencing was performed on an Illumina HiSeq 2500 using traditional Illumina methods (Malone and Oliver, 2011) to generate approximately 50 million reads per sample. Raw reads were mapped to the reference human genome hg19 using TopHat v2.1 (Trapnell et al., 2009). Aligned reads were then imported onto the Avadis NGS analysis platform (Strand life Sciences) and filtered based on read quality followed by read statistics to remove duplicates. Transcript abundance was quantified using the TMM (Trimmed Mean of M-values) algorithm (Dillies et al., 2012; Robinson and Oshlack, 2010) as the normalization method.

Quantification of cellular protein expression

Histopathology reviews were conducted on the whole slide digital images. Protein expression of nuclear factors in α and β cells was quantified using MetaMorph 7.1 imaging software (Molecular Devices) using manual cell counting (Brissova et al., 2014) where an average of 351±73 α cells and 861±141 β cells were counted per normal donor (n=7), and average of 718±50 α cells and 45±17 β cells were counted per T1D donor (n=4) for each transcription factor.

RNA-sequencing analysis

Genes with normalized expression values less than 25 were removed prior to differential expression analysis between control and T1D groups. Fold change (cutoff ≥ ±1.5) was calculated based on p-value estimated by z-score calculations (cutoff 0.05) as determined by Benjamini Hochberg false discovery rate (FDR) correction of 0.05 (Benjamini and Hochberg, 1995). Differentially expressed genes were further analyzed through Ingenuity Pathway Analysis (IPA, Qiagen) (**Figure S4C**, **Table S3**) and Gene Ontology (GO) analysis using DAVID v6.8 (Huang et al., 2009) (**Figures 4B** and **S4D**, **Table S4**).

RESOURCES TABLE

REAGENT or RESOURCE	SOURCE	IDENTIFIER
Antibodies		
Rabbit anti-ARX (1:1000)	Beta Cell Biology Consortium (BCBC)/Patrick Collombat	N/A
Rabbit anti-Glucagon (1:200)	Cell Signaling	Cat# 2760; RRID: AB_659831
Mouse anti-Glucagon (1:500)	Abcam	Cat# ab10988; RRID: AB_297642
Mouse anti-Glucagon- Pacific Blue (1:600; flow cytometry)	Sigma-Aldrich	Cat# G2654; RRID: AB_259852
Rabbit anti-Insulin-647 (1:65)	Cell Signaling	Cat# 9008
Guinea pig anti-Insulin (1:1000)	Dako	Cat# A0564
Chicken anti-Insulin (1:10; flow cytometry)	Gallus Immunotech	Cat# ABI
Rabbit anti-MAFB (1:3000)	Gift from Roland Stein, Vanderbilt University	Cat# BL1228
Mouse anti-NKX2.2 (1:1000)	Developmental Studies Hybridoma Bank	Cat# 74-5A5; RRID: AB_531794
Rabbit anti-NKX6.1 (1:2000)	BCBC/Palle Serup	N/A
Rabbit anti-PDX1 (1:5000)	C. V. E. Wright	N/A
Goat anti-PDX1 (1:5000)	C. V. E. Wright	N/A
Goat anti-Somatostatin (1:500)	Santa Cruz	Cat# sc-7819; RRID: AB_2302603
Mouse anti-Somatostatin-AlexaFluor 488 (1:200; flow cytometry)	LS Bio	Cat# LS-C169129-100
Mouse anti-HIC3-2D12 (Hpa3; 1:200; flow cytometry)	Gift from Drs. Philip Streeter and Markus Grompe	N/A
Mouse anti-HIC0-4F9-Biotin (Hpi1; 1:100; flow cytometry)	Novus	Cat# NBP1-18872B RRID: AB_2126328
Donkey anti-chicken-APC (1:25; flow cytometry)	Jackson ImmunoResearch	Cat #703-136-155 RRID: AB_2340360
Donkey anti-goat-Alexa Flour 647 (1:200)	Jackson ImmunoResearch	Cat #705-605-003 RRID: AB_2340436
Donkey anti-Guinea pig-Cy2 (1:500)	Jackson ImmunoResearch	Cat #706-225-148 RRID: AB_2340467
Donkey anti-Guinea pig-Cy5 (1:200)	Jackson ImmunoResearch	Cat #706-175-148 RRID: AB_2340462
Donkey anti-mouse-Cy5 (1:200)	Jackson ImmunoResearch	Cat #715-175-151 RRID: AB_2340820
Donkey anti-rabbit-Cy3 (1:500)	Jackson ImmunoResearch	Cat #711-165-152 RRID: AB_2307443
Goat anti-mouse-PE (1:1000; flow cytometry)	BD Biosciences	Cat# 550589 RRID: AB_393768
Streptavidin BV421 (1:500; flow cytometry)	BD Biosciences	Cat# 563259
Biological Samples		
Human Pancreatic Islets (control and T1D)	Integrated Islet Distribution Program and Rita Bottino	
Human Pancreatic Tissue (control and T1D)	Rita Bottino	

Chemicals, Peptides, and Recombinant Proteins		
Propidium Iodide	BD Biosciences	Cat# 556463
Exenatide-4 (Ex-4)	California Peptide	Cat# 507-77
L-Arginine monohydrochloride	Sigma Life Science	Cat# A6969-25G; CAS: 001119-34-2
D-(+)-Glucose	Sigma Life Science	Cat# G7528-1KG; CAS: 50-99-7
3-Isobutyl-1-methylxanthine (IBMX)	Sigma Life Science	Cat# I5879-1G; CAS: 28822-58-4
(±)-Epinephrine-hydrochloride	Sigma-Aldrich	Cat# E4642-5G; CAS: 329-63-5
Potassium Chloride	Fisher Scientific	Cat# BP366-500; CAS: 7447-40-7
Collagenase NB1 Premium Grade	Crescent Chemical	Cat# 17455.03
Neutral Protease NB1 Premium Grade	Crescent Chemical	Cat# 30301.02
DNase I	Worthington Biochemical Corporation	Cat# LS006333
RPMI Medium	Mediatech	99-595-CM
Biocoll-Separating Solution, Density 1.10 g/mL	Cedarlane	Cat# L6155
Biocoll-Separating Solution, Density 1.077 g/mL	Cedarlane	Cat# L6113
Fetal Calf Serum	Life Technologies	Cat# 16-140-071
Dithizone	Sigma	Cat# D5130
CMRL 1066 Medium	Mediatech	Cat# 99-663-CV
Penicillin/Streptomycin mix	Life Technologies	Cat# 15140163
L-glutamine	Life Technologies	Cat# 2030-081
16% paraformaldehyde	Electron Microscopy Sciences	Cat# 15710
O.C.T. compound	Fisher Scientific	Cat# 4585
Critical Commercial Assays		
Insulin Radioimmunoassay	Millipore	RI-13K
Glucagon Radioimmunoassay	Millipore	GL-32K
RNAqueous-Microkit	Invitrogen by Thermo Fisher Scientific	AM1931
EIA ELISA	Phoenix Pharmaceuticals	EK-070-94
Human-specific insulin radioimmunoassay	Millipore	HI-14K
Deposited Data		
RNA-seq data for FACS purified human control and T1D alpha cells	NCBI Gene Expression Omnibus	GEO: GSE106148
Experimental Models: Organisms/Strains		
Mouse: NOD-*scid-IL2rγ*^{null} (NSG)	Jackson Laboratory	https://www.jax.org/strain/005557
Oligonucleotides		
18S	Applied Biosystems	Hs99999901_s1
ACTB	Applied Biosystems	Hs99999903_m1
ARX	Applied Biosystems	Hs00292465_m1
GCG	Applied Biosystems	Hs00174967_m1
INS	Applied Biosystems	Hs02741908_m1
MAFA	Applied Biosystems	Hs01651425_s1
MAFB	Applied Biosystems	Hs00534343_s1
NKX2.2	Applied Biosystems	Hs00159616_m1

NKX6.1	Applied Biosystems	Hs00232355_m1
PDX1	Applied Biosystems	Hs00236830_m1
Software and Algorithms		
TopHat (v2.1)	Trapnell, 2009	http://tophat.cbcb.umd.edu/ RRID: SCR_013035
Avadis NGS analysis Platform	Strand life Sciences, Bengaluru	http://www.avadis-ngs.com RRID: SCR_000644
Trimmed Mean of M-values (TMM) algorithm	Dillies, 2012 Robinson, 2010	
DAVID (v6.8)	Huang, 2009	http://david.abcc.ncifcrf.gov/ RRID: SCR_001881
Ingenuity Pathway Analysis (IPA)	Qiagen	RRID: SCR_008653
Prism v.7.0	Graphpad Software	https://www.graphpad.com; RRID: SCR_002798
MetaMorph 7.1	Molecular Devices	https://www.moleculardevices.com; RRID: SCR_002368
Zeiss LSM Imaging Software (confocal)	Carl Zeiss	https://www.zeiss.com; RRID: SCR_014344
Genome Analysis Toolkit (GATK) HaploTypeCaller v3.3	Broad Institute	https://software.broadinstitute.org/gatk/; RRID: SCR_001876
Other		
Zenon Kit Alexa Fluor 488	Invitrogen	Cat# Z25002
Zenon Kit Pacific Blue	Invitrogen	Cat# Z25041
Tyramide Signal Amplification	Perkin Elmer	Cat# NEL744001KT

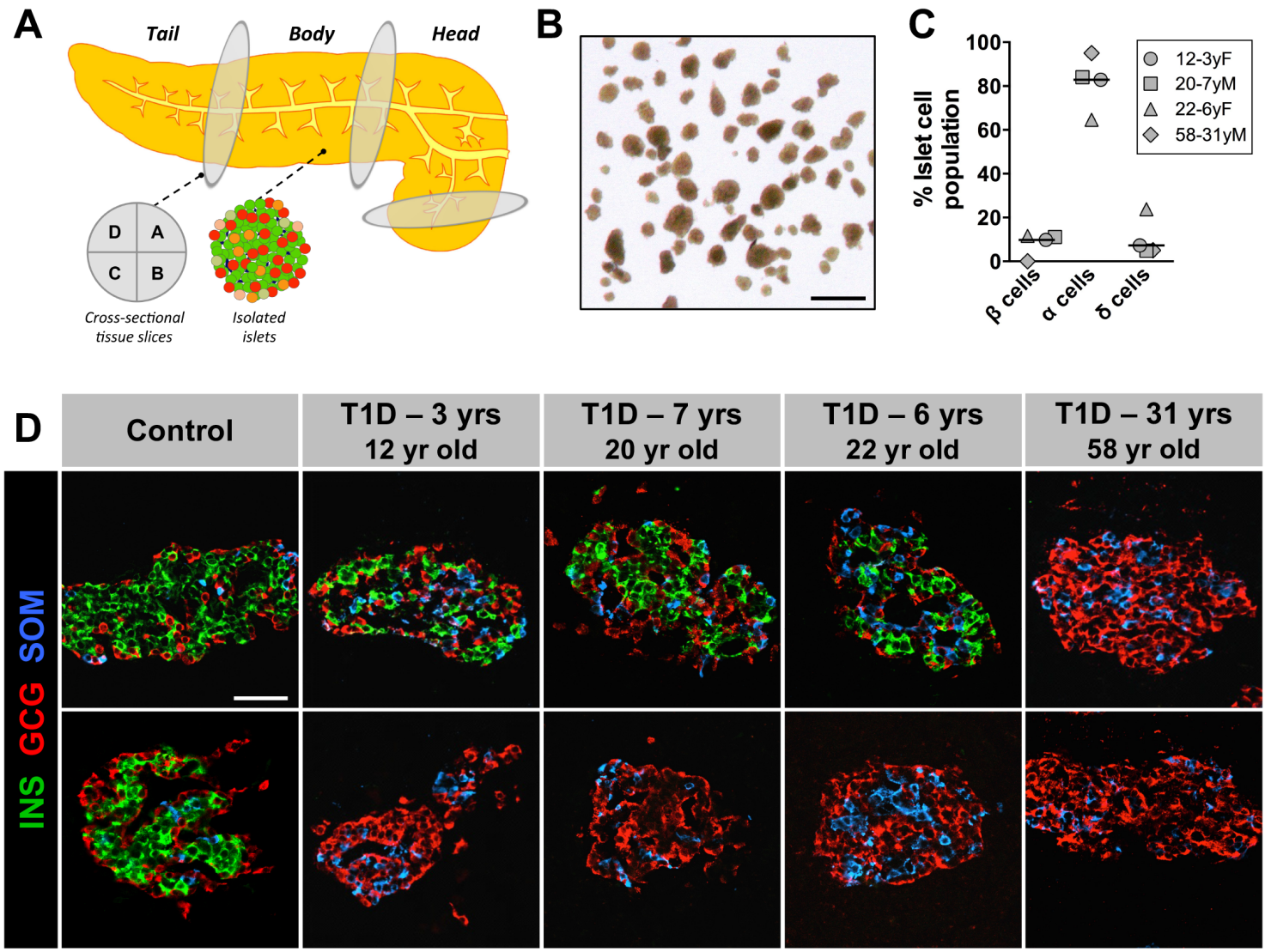

Figure S1. Related to Figures 1 and 2. Composition and morphology in T1D islets. (**A**) Schematic of islet isolation and tissue procurement from the same pancreas. Prior to islet isolation, multiple cross-sectional slices of pancreas with 2-3 mm thickness were obtained from the head, body and tail. Pancreatic slices were further divided into four quadrants (*A, B, C, D*) and processed for histology. (**B**) Pancreatic islets procured from a 12-year-old individual with 3-year T1D duration (donor #1). (**C**) Endocrine cell populations in dispersed isolated islets from 3 donors (#1,4,5) with recent-onset T1D contained 10.8±0.5% β cells, 77.1±6.3% α cells, and 12.0±5.9% δ cells. The donor with longstanding T1D (donor #8) had 0% β cells, 95% α cells, and 5% δ cells. For comparison, islets from normal individuals (n=28) with average age of 36±2 years (range 16 – 63 years) assessed by this approach had 53.4±2.6% β cells, 38.5±2.7% α cells, and 7.5±0.9% δ cells (Blodgett et al., 2015). (**D**) Morphology of T1D islets in the native pancreas. On average 250 islets from pancreatic head, body and tail of each T1D donor were analyzed for the presence of β cells. An islet was categorized as insulin+ even if it had only one insulin-positive cell. The number of insulin+ islets varied in 4 donors (#1,3,4,5) with recent-onset T1D (17.8±15.5%), but no insulin+ islets were found in the pancreatic sections of our longstanding cases (donors #6,7,8). If donors had insulin+ islets, representative islets are displayed in row 1. INS–insulin, GCG–glucagon, SOM–somatostatin. Scale bar is 50 μm.

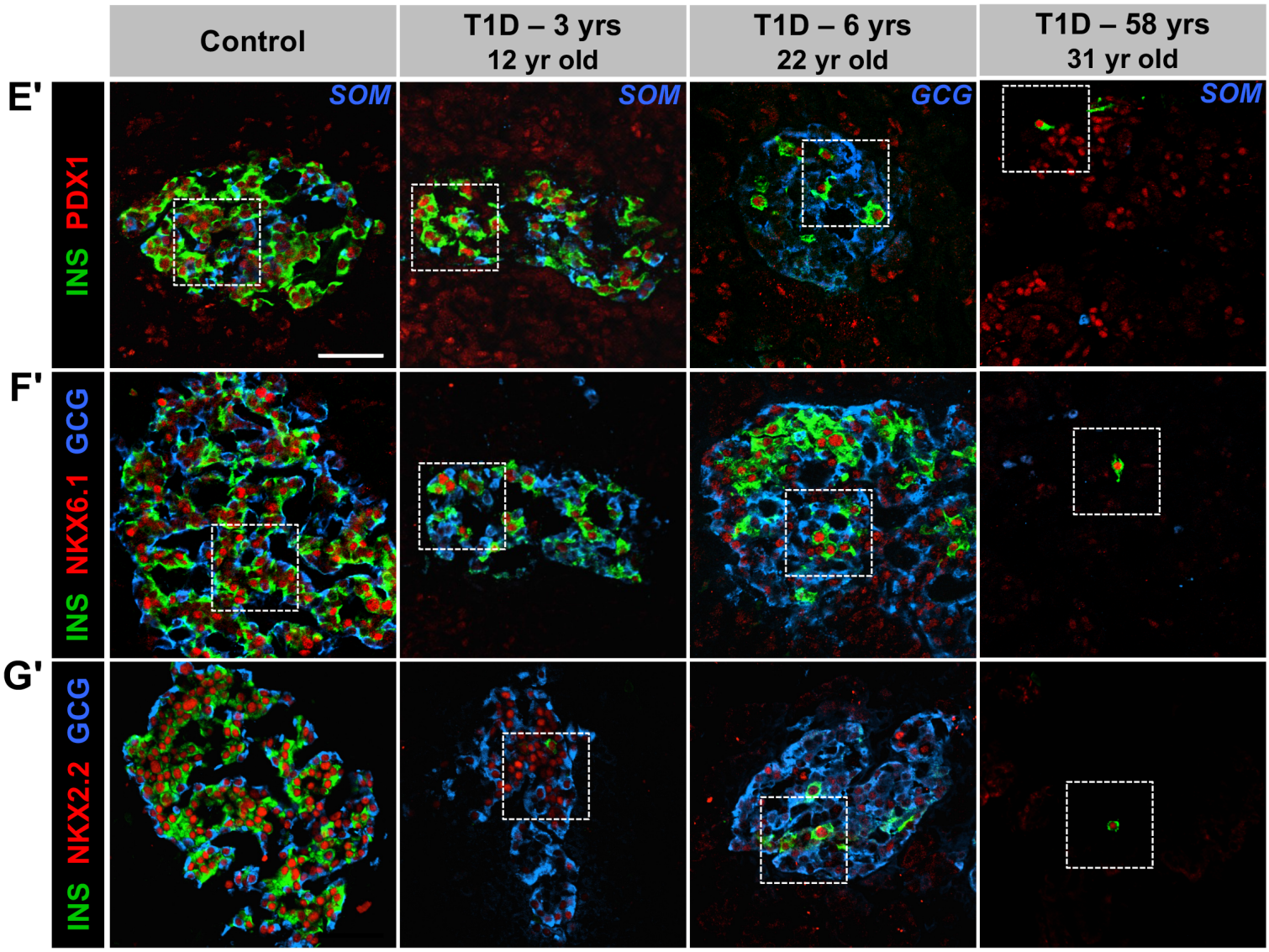

Figure S2. Related to Figure 1. Expression pattern of PDX1, NKX6.1, and NKX2.2 in T1D β cells. Expression of β cell-enriched transcription factors in the native pancreatic tissue from donors with recent-onset T1D (donors #1,5) was compared to 58-year-old donor with 31 years of T1D duration (donor #8) and controls. INS–insulin, GCG–glucagon, SOM–somatostatin. Regions denoted by the dashed line in panels **E'**– **G'** are displayed in panels **E** – **G** in **Figure 1**, respectively. Scale bar in **E'** is 50 μm and also corresponds to panels **F'** and **G'**.

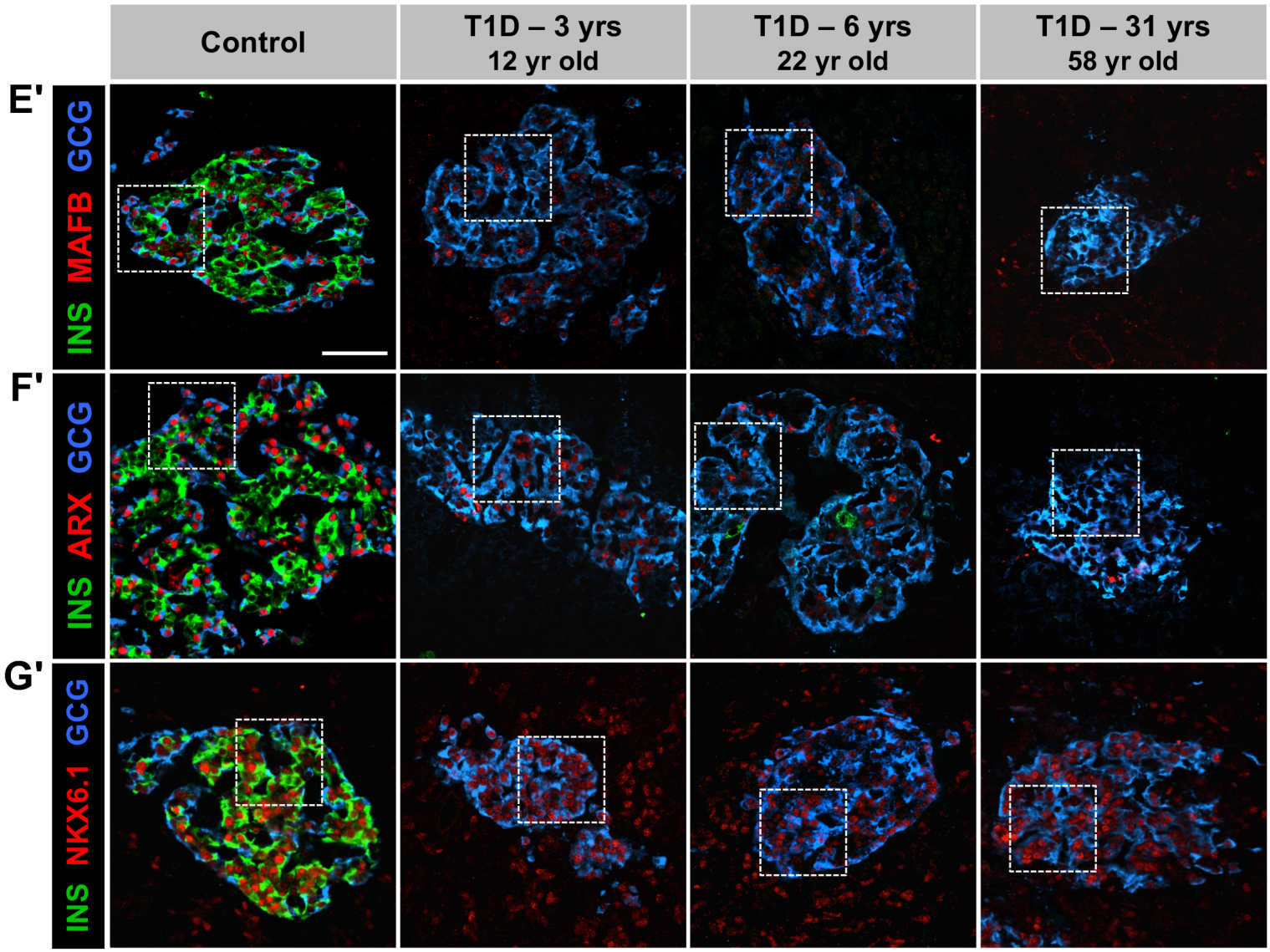

Figure S3. Related to Figure 2. Expression pattern of MAFB, ARX, and NKX6.1 in T1D α cells. Expression of α cell-enriched transcription factors in the native pancreatic tissue from donors with recent-onset T1D (donors #1,2,5) was compared to 58-year-old donor with 31 years of T1D duration and controls (donor #8). GCG–glucagon, SOM–somatostatin. Regions denoted by the dashed line in panels **E'**–**G'** are displayed in panels **E**–**G** in **Figure 2**, respectively. Scale bar in **E'** is 50 μm and also corresponds to panels **F'** and **G'**.

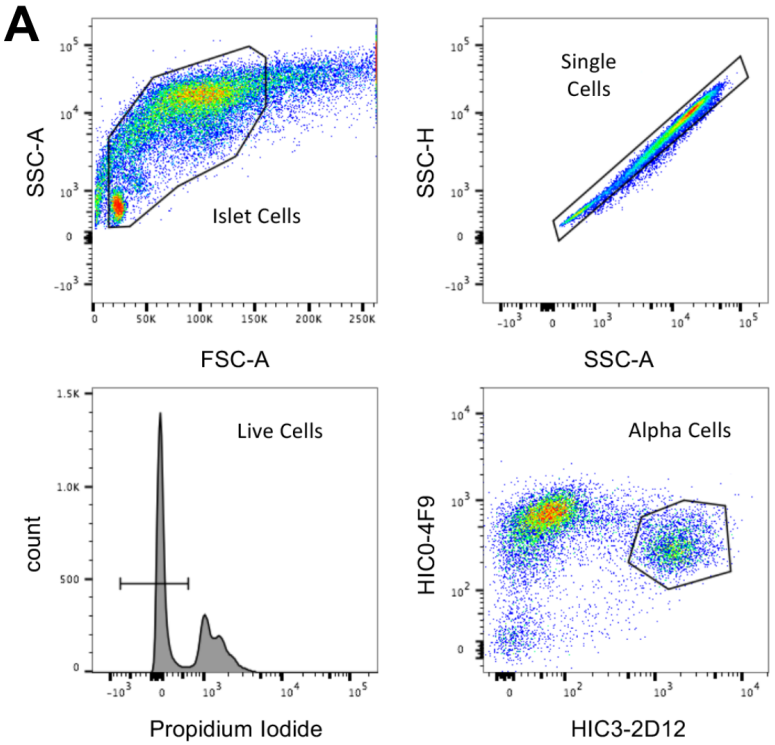
A
SSC-A
FSC-A
Islet Cells
SSC-H
SSC-A
Single Cells
count
Propidium Iodide
Live Cells
HIC0-4F9
HIC3-2D12
Alpha Cells

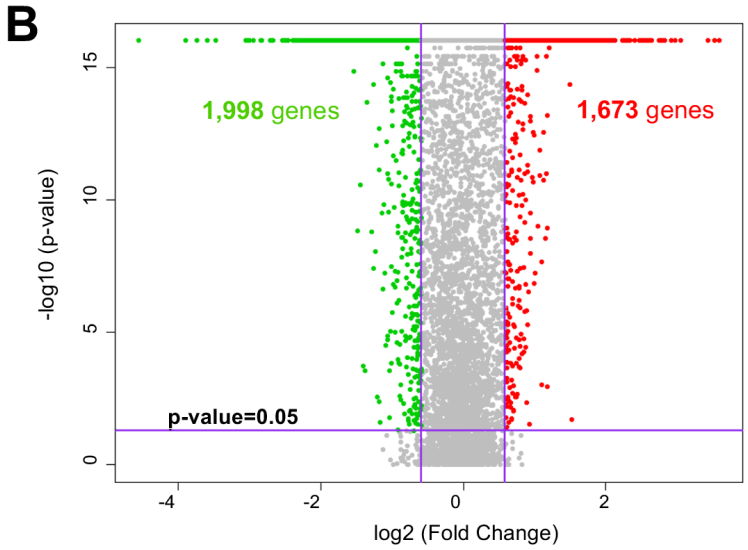
B
-log10 (p-value)
log2 (Fold Change)
1,998 genes
1,673 genes
p-value=0.05

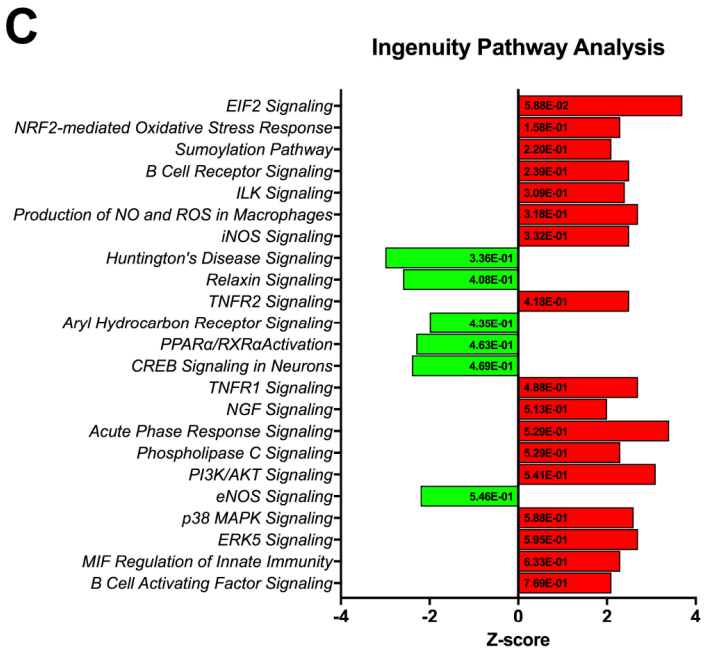
C
Ingenuity Pathway Analysis
EIF2 Signaling
NRF2-mediated Oxidative Stress Response
Sumoylation Pathway
B Cell Receptor Signaling
ILK Signaling
Production of NO and ROS in Macrophages
iNOS Signaling
Huntington's Disease Signaling
Relaxin Signaling
TNFR2 Signaling
Aryl Hydrocarbon Receptor Signaling
PPARα/RXRαActivation
CREB Signaling in Neurons
TNFR1 Signaling
NGF Signaling
Acute Phase Response Signaling
Phospholipase C Signaling
PI3K/AKT Signaling
eNOS Signaling
p38 MAPK Signaling
ERK5 Signaling
MIF Regulation of Innate Immunity
B Cell Activating Factor Signaling
5.88E-02
1.58E-01
2.20E-01
2.39E-01
3.09E-01
3.18E-01
3.32E-01
3.36E-01
4.08E-01
4.18E-01
4.35E-01
4.63E-01
4.69E-01
4.88E-01
5.13E-01
5.29E-01
5.29E-01
5.41E-01
5.46E-01
5.88E-01
5.95E-01
6.33E-01
7.69E-01
Z-score

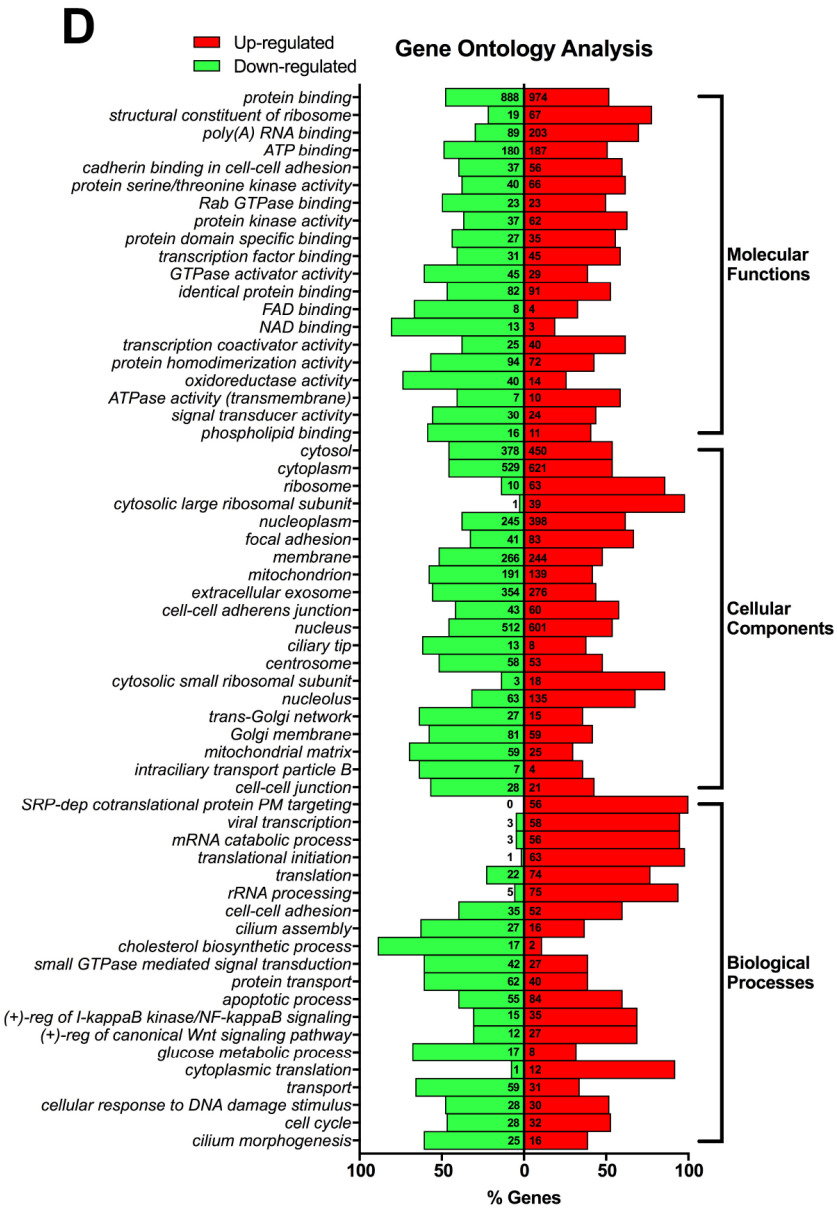
D
Up-regulated
Down-regulated
Gene Ontology Analysis
protein binding
structural constituent of ribosome
poly(A) RNA binding
ATP binding
cadherin binding in cell-cell adhesion
protein serine/threonine kinase activity
Rab GTPase binding
protein kinase activity
protein domain specific binding
transcription factor binding
GTPase activator activity
identical protein binding
FAD binding
NAD binding
transcription coactivator activity
protein homodimerization activity
oxidoreductase activity
ATPase activity (transmembrane)
signal transducer activity
phospholipid binding
cytosol
cytoplasm
ribosome
cytosolic large ribosomal subunit
nucleoplasm
focal adhesion
membrane
mitochondrion
extracellular exosome
cell-cell adherens junction
nucleus
ciliary tip
centrosome
cytosolic small ribosomal subunit
nucleolus
trans-Golgi network
Golgi membrane
mitochondrial matrix
intraciliary transport particle B
cell-cell junction
SRP-dep cotranslational protein PM targeting
viral transcription
mRNA catabolic process
translational initiation
translation
rRNA processing
cell-cell adhesion
cilium assembly
cholesterol biosynthetic process
small GTPase mediated signal transduction
protein transport
apoptotic process
(+)-reg of I-kappaB kinase/NF-kappaB signaling
(+)-reg of canonical Wnt signaling pathway
glucose metabolic process
cytoplasmic translation
transport
cellular response to DNA damage stimulus
cell cycle
cilium morphogenesis
Molecular Functions
Cellular Components
Biological Processes
% Genes

Figure S4. Related to Figure 4. Transcriptome analysis of purified human α cells by RNA-sequencing. (**A**) Gating strategy for sorting of dispersed human islet cells by Fluorescence Activated Cell Sorting (FACS). Cell debris was excluded by forward scatter (FSC) and side scatter (SSC), single cells were identified by SSC-H v. SSC-A plot, and non-viable cells were excluded using Propidium Iodide (PI). The α cell population was isolated based on double positivity for HIC3-2D12 (Hpa3) and HIC0-4F9 (Hpi1) antibodies. (**B**) Volcano plot displays transcripts differentially expressed between control and T1D samples (donors #3,6,7) that reached statistical significance (upregulation: red; downregulation: green). Differential expression between the two sample sets was calculated on the basis of FC (≥1.5) with a <0.05 p-value cut-off for calculated z-score. (**C**) Graph represents the top 20 most significantly (z-score >2 or <-2) altered canonical pathways identified by Ingenuity Pathway Analysis (IPA) with corresponding p-value depicted on graph bar. Pathways with affiliated Ensembl Gene Stable IDs are listed in **Table S3**. (**D**) Bar graph highlights the percentage of up- and down-regulated genes (with corresponding gene number displayed within bar) in the top 20 significant biological processes, cellular components, and molecular functions identified by Gene Ontology (GO) term analysis. Corresponding p-values, Ensembl Gene Stable IDs and process GO accession numbers are listed in **Table S4.**

Table S1. Related to Figures 1-4. Demographic information of normal donors

Donors	Age (years)	Ethnicity/ Race	Gender	BMI	Cause of Death	Tissue/Islet Source
Normal Controls for Islet Perifusion	7	Caucasian	M	26.8	Respiratory arrest	Rita Bottino
	8	Caucasian	F	16.1	Intracerebral hemorrhage	Rita Bottino
	8	African American	M	17.2	Anoxia	Rita Bottino
	9	Caucasian	M	15.5	Head Trauma	Rita Bottino
	11	African American	M	18.3	Anoxia	Rita Bottino
	19	Caucasian	M	20.1	Head Trauma	Rita Bottino
	19	Caucasian	M	34.1	Head Trauma	IIDP
Normal Controls for Islet Transplants	20	African American	M	21.7	Head Trauma	IIDP
	39	N/A	F	28.2	N/A	IIDP
	53	Native Hawaiian or Other Pacific Islander	F	25.4	N/A	IIDP
Normal Control for qRT-PCR	11	Caucasian	M	22.7	Anoxia	Rita Bottino
	20	Hispanic/ Latino	F	24.6	Anoxia	IIDP
	29	Hispanic/ Latino	M	27.5	Head Trauma	IIDP
Normal Controls for Histology	8	African American	M	17.2	Anoxia	Rita Bottino
	10	Caucasian	M	19.3	Head Trauma	Rita Bottino
	19	Caucasian	M	20.1	Head Trauma	Rita Bottino
	19	Caucasian	M	21.2	Anoxia	Rita Bottino
	20	Hispanic/ Latino	M	19.4	Head Trauma	Rita Bottino
	24	Caucasian	M	35.5	Head Trauma	Rita Bottino
	55	African American	M	35.6	Stroke	Rita Bottino
Normal Controls for RNA-seq	26	Hispanic/Latino	F	35.9	Anoxia	IIDP
	35	Caucasian	F	23.6	Anoxia	IIDP
	49	Caucasian	F	31.6	Stroke	IIDP
	50	African American	M	30.2	Stroke	IIDP
	55	Caucasian	M	27.8	Stroke	IIDP

N/A – not available; IIDP – Integrated Islet Distribution Program

Table S2. Related to Figures 1- 4 and Table 1. DNA sequencing of T1D donors for variants associated with monogenic diabetes

Donor	Gene	Chr	Transcript	Nucleotide	Amino Acid Change	dbSNP ID	MAF	POLY Score
1	*AKT2*	19	NM_001626.5	c.*9C>T	-	rs79275829	0.004	0
	CYP27B1	12	NM_000785.3	c.963+2T>G	-	-	0	0
	CYP27B1	12	NM_000785.3	c.963+7T>G	-	-	0	0
	FOXP3	X	NM_014009.3	c.403A>C	p.Thr135Pro	-	0	0
	IFIH1	2	NM_022168.3	c.1641+1G>C	-	rs35337543	0.007	0
	SIRT1	10	NM_012238.4	c.110C>T	p.Pro37Leu	-	0	0.013
	GLP1R	6	NM_002062.3	c.1347G>A	p.Ala449Ala	rs201020486	0	0
2	*AIRE*	21	NM_000383.3	c.1411C>T	p.Arg471Cys	rs74203920	0.006	0.997
	ALMS1	2	NM_015120.4	c.69_77del	p.Glu27_Glu29del	-	0	0
	HSD11B1	1	NM_005525.3	c.219+6G>A	-	rs202219444	0	0
	LRBA	4	NM_006726.4	c.1536A>G	p.Ser512Ser	-	0	0
	POMC	2	NM_001035256.1	c.706C>G	p.Arg236Gly	rs28932472	0.004	1
	PTPN22	1	NM_015967.5	c.1508A>G	p.Tyr503Cys	rs371916399	0	0.004
	TBC1D4	13	NM_014832.3	c.2913A>T	p.Gly971Gly	rs184774790	0	0
3	*BBS5*	2	NM_152384.2	c.620G>A	p.Arg207His	rs35487251	0.006	0.833
	BLM	15	NM_000057.3	c.2119C>T	p.Pro707Ser	rs146077918	0.001	0.018
	EIF2AK3	2	NM_004836.5	c.-201A>G	-	rs144057685	0.005	0
	HFE	6	NM_000410.3	c.845G>A	p.Cys282Tyr	rs1800562	0.02	0
	HNF4A	20	NM_175914.4	c.1314C>G	p.Leu438Leu	-	0	0
	PIK3R1	5	NM_181523.2	c.1176C>T	p.Phe392Phe	rs3730090	0.308	0
4	*ALMS1*	2	NM_015120.4	c.12278G>A	p.Arg4093His	-	0	0
	FBN1	15	NM_000138.4	c.3294C>T	p.Asp1098Asp	rs140587	0.008	0
	GLP1R	6	NM_002062.3	c.59G>A	p.Arg20Lys	rs10305421	0.007	0.643
	IFIH1	2	NM_022168.3	c.1075G>C	p.Val359Leu	-	0	0.996
	MKS1	17	NM_017777.3	c.1528C>T	p.Arg510Trp	-	0	0.976

5	*BLM*	15	NM_000057.3	c.2268A>G	p.Lys756Lys	rs146013879	0.001	0
	CLEC16A	16	NM_015226.2	c.2945G>A	p.Ser982Asn	rs72650689	0.004	0.967
	HFE	6	NM_000410.3	c.187C>G	p.His63Asp	rs1799945	0.084	0
	LRBA	4	NM_006726.4	c.7597A>C	p.Thr2533Pro	rs62346982	0.003	0.167
	KCNK16	6	NM_032115.3	c.165G>A	p.Leu55Leu	rs138076469	0.002	0
	LMNA	1	NM_005572.3	c.612G>A	p.Leu204Leu	rs12117552	0.004	0
6	*ABCC8*	11	NM_000352.4	c.-430C>T	-	-	0	0
	BBS2	16	NM_031885.3	c.155T>A	p.Val52Asp	-	0	0.016
	EIF2AK3	2	NM_004836.5	c.-201A>G	-	rs144057685	0.005	0
	MKKS	20	NM_018848.3	c.1015A>G	p.Ile339Val	rs137853909	0.001	0.008
	NTRK2	9	NM_006180.4	c.483T>G	p.Thr161Thr	rs199849633	0	0
	VPS13B	8	NM_017890.4	c.8978A>G	p.Asn2993Ser	rs28940272	0.002	0.997
7	*ABCC8*	11	NM_000352.4	c.2176G>A	p.Ala726Thr	rs138687850	0.001	0.02634
	AKT2	19	NM_001626.5	c.1110G>T	p.Pro370Pro	rs41309435	0.001	0
	CFTR	7	NM_000492.3	c.1521_1523del	p.Phe508del	rs199826652	0.006	0
	LRBA	4	NM_006726.4	c.217-10del	-	-	0	0
	VPS13B	8	NM_017890.4	c.1832G>A	p.Arg611Lys	rs61754109	0	0.02634
8	*AKT2*	19	NM_001626.5	c.945G>A	p.Glu315Glu	rs150000674	0.002	0
	CYP27B1	12	NM_000785.3	c.963+2T>G	-	-	0	0
	CYP27B1	12	NM_000785.3	c.963+7T>G	-	-	0	0
	FXN	9	NM_000144.4	c.-7G>A	-	rs145006100	0.011	0
	IFIH1	2	NM_022168.3	c.1641+1G>C	-	rs35337543	0.007	0

Chr – Chromosome, MAF – Minor allele frequency; DNA isolated from pancreatic samples of T1D donors was subjected to DNA sequencing covering coding regions and splice junctions of 148 genes associated with monogenic diabetes.

SUPPLEMENTAL REFERENCES

Aamodt, K.I. et al., 2016. Development of a reliable automated screening system to identify small molecules and biologics that promote human β-cell regeneration. *American journal of physiology Endocrinology and metabolism*, 311(5), pp.E859–E868.

Alkorta-Aranburu, G. et al., 2016. Improved molecular diagnosis of patients with neonatal diabetes using a combined next-generation sequencing and MS-MLPA approach. *Journal of pediatric endocrinology & metabolism : JPEM*, 29(5), pp.523–531.

Benjamini, Y. & Hochberg, Y., 1995. A direct approach to false discovery rates. *J. Royal Stat. Soc., Ser. B*, 57(1), pp.289–300.

Blodgett, D.M. et al., 2015. Novel Observations From Next-Generation RNA Sequencing of Highly Purified Human Adult and Fetal Islet Cell Subsets. *Diabetes*, 64(9), pp.3172–3181.

Brissova, M. et al., 2014. Islet microenvironment, modulated by vascular endothelial growth factor-A signaling, promotes β cell regeneration. *Cell metabolism*, 19(3), pp.498–511.

Dillies, M.-A. et al., 2012. A comprehensive evaluation of normalization methods for Illumina high-throughput RNA sequencing data analysis. *Briefings in bioinformatics*.

Dorrell, C. et al., 2016. Human islets contain four distinct subtypes of β cells. *Nature communications*, 7, p.11756.

Huang, D.W. et al., 2009. Extracting biological meaning from large gene lists with DAVID. *Current protocols in bioinformatics*, Chapter 13, p.Unit 13.11.

Kayton, N.S. et al., 2015. Human islet preparations distributed for research exhibit a variety of insulin-secretory profiles. *American journal of physiology Endocrinology and metabolism*, 308(7), pp.E592–602.

Malone, J.H. & Oliver, B., 2011. Microarrays, deep sequencing and the true measure of the transcriptome. *BMC biology*, 9, p.34.

Robinson, M.D. & Oshlack, A., 2010. A scaling normalization method for differential expression analysis of RNA-seq data. *Genome biology*, 11(3), p.R25.

Trapnell, C., Pachter, L. & Salzberg, S.L., 2009. TopHat: discovering splice junctions with RNA-Seq. *Bioinformatics (Oxford, England)*, 25(9), pp.1105–1111.